ORGANIC PROCESS RESEARCH & DEVELOPMENT
OPR&D

pubs.acs.org/OPRD

Article

Synthesis of Rovafovir Etalafenamide (Part III): Evolution of the Synthetic Process to the Phosphonamidate Fragment

Andrea Ambrosi,* Dustin A. Bringley, Selcuk Calimsiz, Jeffrey A. O. Garber, Huy Huynh, Sankar Mohan, Keshab Sarma, Jinyu Shen, Jonah Curl, Bernard Kwong, Olga Lapina, Edmund Leung, Lennie Lin, Andrew Martins, Teague McGinitie, Jaspal Phull, Ben Roberts, Mary Rosario, Bing Shi, Eric A. Standley, Li Wang, Xueqing Wang, and Guojun Yu

Cite This: *Org. Process Res. Dev.* 2021, 25, 1247−1262

Read Online

ACCESS | Metrics & More | Article Recommendations | Supporting Information

ABSTRACT: Phosphonamidate **1** is a key fragment in the assembly of rovafovir etalafenamide, a novel nucleotide reverse transcriptase inhibitor under development at Gilead Sciences for the treatment of HIV infection. An early manufacturing route, relying on simulated moving bed (SMB) chromatography for the separation of phosphorus diastereomers, was executed on scale to produce multiple batches of **1**. However, developing alternative synthetic conditions became desirable in consideration of the high production cost, long lead time, and high process mass intensity (PMI) associated with SMB. Several strategies to improve these factors are described herein, including epimerization and recycling of the undesired (*R*)-phosphorus diastereomer, design of stereoselective approaches to establish the desired (S)-configuration at phosphorus, and identification of conditions or derivatives to allow for selective crystallization. Ultimately, a second-generation route to **1** was developed and demonstrated on scale. The new route achieves the separation of phosphorus diastereomers by means of selective crystallization, does not require SMB, and offers lower PMI, cost, and lead time.

KEYWORDS: *phosphonamidate, phosphorus, stereochemistry, SMB, crystallization*

1. INTRODUCTION

Phosphonamidate prodrugs have been part of the medicinal chemistry toolbox since the early 1990s, when McGuigan and co-workers pioneered the ProTide (pronucelotide) strategy to improve the bioavailability and potency relative to the parent phosphonic acids.[1] Within this context, the prodrug tenofovir alafenamide fumarate (TAF, **4**, Figure 1), a nucleotide reverse transcriptase inhibitor (NRTI) approved for the treatment of HIV and HBV infections, represents an example of successful phosphonamidate prodrug implementation,[2] achieving improved properties compared to the phosphonic acid backbone tenofovir (**2**) and the phosphonate diester prodrug tenofovir disoproxyl fumarate (TDF, **3**). Similarly, structure−activity relationship studies demonstrated that the phosphonamidate prodrug rovafovir etalafenamide (GS-9131, **6**) possesses enhanced oral bioavailability and in vitro activity relative to its precursor **5** and other prodrug moieties.[3] The favorable pharmacokinetic profile of rovafovir etalafenamide, along with its unique activity against NRTI-resistant HIV-1 strains, prompted its clinical development at Gilead Sciences.

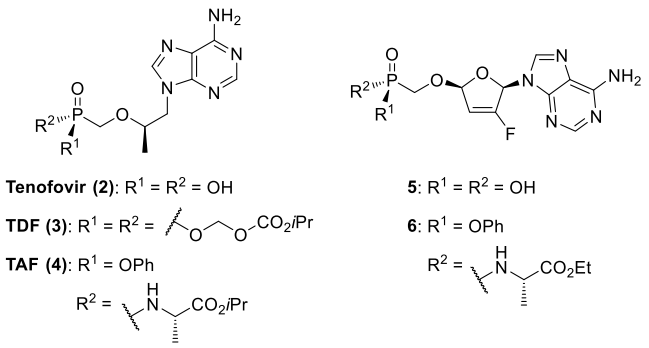

Figure 1. Phosphonamidate prodrugs.

Our retrosynthetic approach to **6** (Scheme 1) involves disconnection to the phosphonamidate fragment **1** and the

Scheme 1. Retrosynthetic Approach to 6

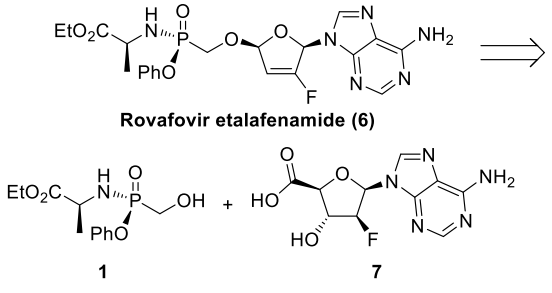

Received: September 25, 2020
Published: May 5, 2021

Scheme 2. First-Generation Route to Phosphonamidate 1

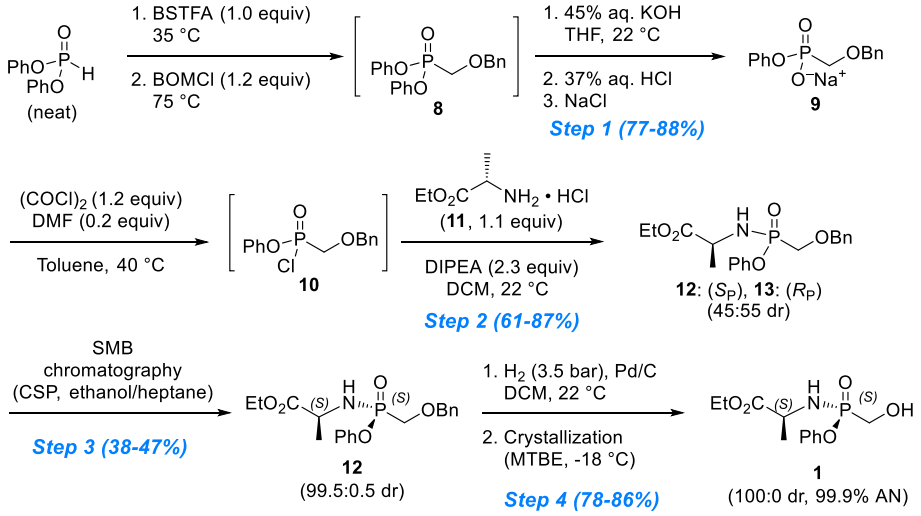

Scheme 3. Epimer Recycling Strategy

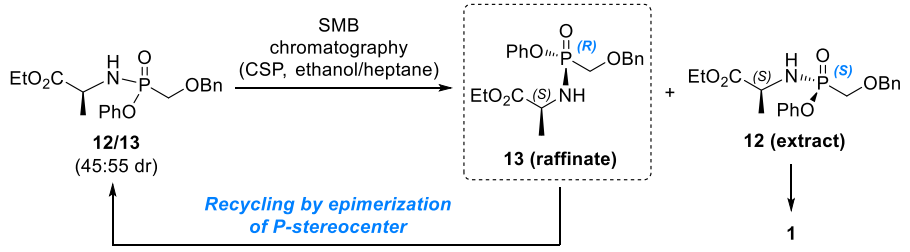

adenosine core **7**. A preceding paper details the assembly of **6** from **1** and **7**.[4] Herein, we describe the evolution of the synthetic process to phosphonamidate **1** from its inception, requiring chromatographic separation of phosphorus diastereomers, to a more efficient, second-generation variant relying on selective crystallization.

The original synthetic route to **1** is shown in Scheme 2.[5] Silylation of diphenylphosphite with *N*,*O*-bis(trimethylsilyl)-trifluoroacetamide (BSTFA), followed by alkylation with benzyloxymethyl chloride (BOMCl) delivered intermediate **8**, which was monohydrolyzed and isolated as the sodium salt **9** in a fully telescoped sequence (77−88% overall yield). Conversion of **9** to the phosphonochloridate **10** and displacement by L-alanine ethyl ester (**11**) afforded a 45:55 mixture of phosphorus epimers **12** and **13** favoring the undesired (R_P)-isomer (61−87% yield). The diastereomers were separated by simulated moving bed (SMB) chromatography on chiral stationary phase (CSP) to furnish the desired (S_P)-diastereomer **12** (99.5:0.5 dr, 38−47% yield) as an ethanolic solution. Finally, hydrogenolysis of the benzyl-protecting group and crystallization from methyl *tert*-butyl ether (MTBE) delivered **1** (78−86% yield) as a single diastereomer in >99% area-normalized (AN) purity.

This sequence was executed on manufacturing scale to produce multiple batches of **1** in 22% overall yield (four steps). However, as the demand for material increased, several issues associated with the synthetic route became apparent. First, reliance on SMB for the separation of diastereomers (step 3) was identified as a major contributor to high cost, process mass intensity (PMI),[6] and long lead time in the production of **1**. It was estimated that SMB accounts for 36% of the production time and 20% of the total PMI, considering all solvents required for the chromatographic separation itself and solvents/water needed for solvent exchange operations from step 2 [dichloromethane (DCM)/toluene to ethanol] to step 4 (ethanol to DCM). Second, the BOMCl alkylation step (step 1) turned out to be sensitive to the quality of the electrophile and often required additional charges to reach full conversion. Third, the intermediates involved in the displacement reaction (step 2) were found to be highly susceptible to hydrolytic degradation, thus requiring strictly anhydrous conditions to prevent the formation of impurities.

Overall, these factors limited the scalability of the process and revealed the need for alternative conditions to reduce cost and lead time. Our research initially focused on developing a recycling strategy to recover the unwanted isomer **13** from SMB separation, hence improving the overall yield and reducing the cost of the current process. Concurrently, in an effort to remove SMB altogether to reduce the lead time, stereoselective synthesis and selective crystallization were investigated as alternatives. These endeavors culminated in the design of a more efficient SMB-free second-generation route that overcomes the previously identified shortcomings.

2. RESULTS AND DISCUSSION

2.1. Recycling Strategy Applied to the Current Process. The undesired (R_P)-isomer **13** is obtained by SMB separation of a nearly 1:1 mixture of phosphorus epimers as a 40−60 wt % ethanolic solution (raffinate, Scheme 3). In previous manufacturing campaigns, this material was discarded, thereby contributing to low overall yield and high waste burden. To increase the efficiency of the synthetic route, the recycling of **13** via P-epimerization was examined.

https://doi.org/10.1021/acs.oprd.0c00428
Org. Process Res. Dev. 2021, 25, 1247−1262

Table 1. Optimization of Epimerization Reaction Conditions

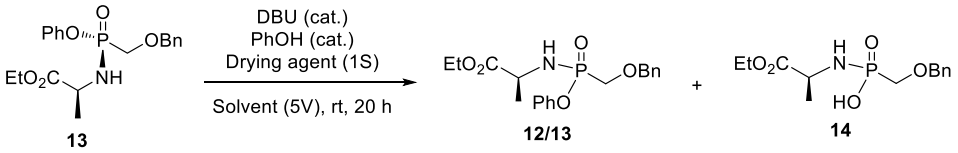

	conditions				results (% AN)[a]		
entry	DBU (mol %)	PhOH (mol %)	solvent	drying agent	**12**	**13**	**14** + PhOH
1		SMB raffinate			0.8	65.9	27.0
2	20	10	DCM		21.1	21.4	52.8
3	20	10	DCM	4 Å MS powder	28.2	28.3	39.9
4	20	10	DCM	4 Å MS beads	27.0	27.1	41.9
5	20	10	DCM	BSA	1.2	58.5	36.1
6	20	10	THF	4 Å MS powder	27.4	29.4	40.4
7	20	10	toluene	4 Å MS powder	29.0	31.6	36.4
8	5	5	DCM	4 Å MS powder	19.7	43.7	32.0
9	10	5	DCM	4 Å MS powder	30.7	33.0	32.0
10	20	5	DCM	4 Å MS powder	31.2	31.2	33.1
11	5		DCM	4 Å MS powder	11.9	54.1	28.4
12	10		DCM	4 Å MS powder	32.2	34.9	29.1
13	**20**		**DCM**	**4 Å MS powder**	**32.7**	**32.6**	**29.0**

[a]Determined by UPLC−MS.

Previous studies with compound **S1** had identified the combination of catalytic amounts of 1,8-diazabicyclo[5.4.0]-undec-7-ene (DBU) and phenol in the presence of a drying agent as suitable conditions for epimerization at phosphorus (see Supporting Information). These conditions were used as the starting point to further optimize the epimerization of **13**.

The raffinate was received as a solution in ethanol from SMB separation, with **13** accounting for 65.9% AN of the mixture composition and in 98.8:1.2 dr (Table 1, entry 1). The raffinate also contained a mixture of phenol and **14**[7] [inseparable by ultraperformance liquid chromatography (UPLC) analysis] amounting to 27.0% AN. Given the incompatibility of **13** with a mixture of alcohol and base (which would lead to the displacement of phenol by the alcohol), solvent exchange from ethanol to a suitable reaction solvent was necessary prior to the initiation of the epimerization reaction. Screening of drying agents and solvents (entries 2−7) identified DCM and 4 Å powder molecular sieves as a suitable combination to reach a 1:1 mixture of isomers with little loss to hydrolysis (entry 3). Omission of drying agents resulted in a higher loss to hydrolysis (entry 2). After further optimization of these conditions, it was determined that 20 mol % DBU allows to reach equilibrium as a 1:1 mixture within 20 h (entries 11−13). Additionally, the amount of phenol has little impact on the reaction outcome (entries 3, 10, and 13), as some phenol (typically 5−10 mol %) is already present in the SMB raffinate.

A 50 g scale experiment was carried out to assess the scalability of the optimized conditions (Scheme 4). The ethanolic SMB raffinate containing **13** was first diluted with DCM (2 V) and washed with water (3 × 2 V) to remove ethanol completely. The resulting DCM solution was treated with 4 Å powder molecular sieves (0.5 S) and subjected to the epimerization conditions. The reaction provided **12**/**13** in 96% yield as a 47:53 mixture of diastereomers after work-up.

Scheme 4. Optimized Reaction Conditions for P-Epimerization

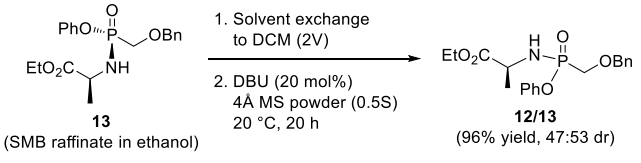

Two limiting mechanisms can be envisioned for P-epimerization of phosphonamidates (Figure 2):[8] (i) a dissociative, elimination−addition mechanism by deprotonation at nitrogen and ejection of phenolate, proceeding through metaphosphonimidate **i**, and (ii) an associative, S_N2-type mechanism by direct nucleophilic attack at phosphorus of phenolate (formed from phenol and base) or nucleophilic base, proceeding through the pentacoordinate intermediate or transition state **ii**.[9] Experimental evidence gathered over the course of these studies suggests that the former hypothesis is more plausible (Table 2). In addition to DBU, epimerization also proceeds in the presence of guanidine bases ($pK_{a\ BH+} > 16$, entries 1−3) but not with tertiary amines or other weaker bases ($pK_{a\ BH+} < 15$, entries 5−7). The pK_a value of the conjugate acid, rather than its nucleophilicity, seems to be the determining factor. Moreover, epimerization does not proceed with the *N*-benzyl derivative **15** (entry 4), where deprotonation at nitrogen is not possible. These observations support an elimination−

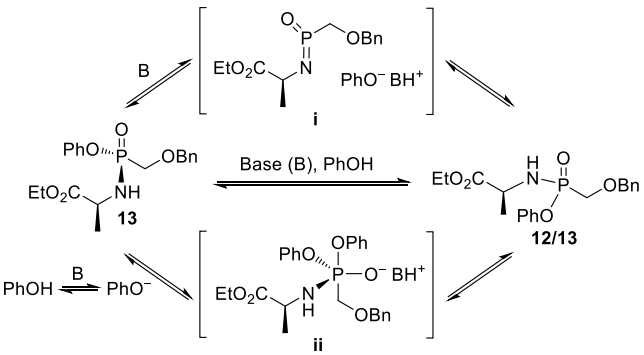

Figure 2. Epimerization mechanisms.

https://doi.org/10.1021/acs.oprd.0c00428
Org. Process Res. Dev. 2021, 25, 1247−1262

Table 2. Impact of Base Selection on the Epimerization Reaction

Entry	Base	$pK_{a\,BH^+}$ (in THF)	Epimerization
1	 TBD	21.0[a]	✓
2	 MTBD	17.9[a]	✓
3	 DBU	16.8[a]	✓
4[e]			×
5	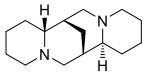 (−)-Sparteine	14.3[b]	×
6	Et_3N	13.7[c]	×
7	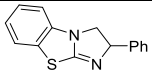 Benzotetramisole	N/A[d]	×

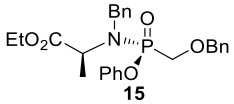
15

[a]Reference 10a. [b]Reference 10b. [c]Reference 10c. [d]pK_a values for isothioureas are in the 7.3−10.3 range (ref 11). [e]Substrate **15** was used.

association mechanism through metaphosphonimidate **i**, with the consequent loss of stereochemical information.

2.2. Stereoselective Synthesis. The development of stereoselective methods to access phosphoric/phosphonic acid derivatives as single isomers has been largely stimulated by the well-established influence of the phosphorus configuration on biological activity.[3a,12,13] The existing stereoselective methods rely on a chiral auxiliary,[14] enzymatic kinetic resolution,[15] dynamic kinetic asymmetric transformation (DYKAT)[16] of a configurationally labile intermediate,[13,17] organocatalysis,[18] or stereospecific displacement on a stereodefined substrate.[19] In an effort to avoid physical methods of separation (either chromatography or crystallization), we investigated the possibility of synthesizing **1** stereoselectively by means of chiral auxiliary and/or DYKAT strategies.

Previously, the investigation of the stereoselective synthesis of **4** had revealed the possibility of establishing the desired configuration at phosphorus via crystallization-induced asymmetric transformation (CIAT)[20] of a configurationally labile phosphonochloridate intermediate. As **1** possesses the same stereochemical arrangement at the phosphorus atom as **4**, we envisioned that, by installing a benzimidazole-derived chiral auxiliary (**16**, Scheme 5) as a surrogate of the chiral adeninopropanol chain in **4**, a similar CIAT process could be accessed during chlorination to provide diastereomerically enriched **18**. The benzimidazole moiety was chosen to potentially impart crystallinity to the phosphonochloridate intermediate **17**. Moreover, the presence of a phenyl group would aid the cleavage of the chiral auxiliary by hydrogenolysis in the final step.

Substrate **16** was synthesized in six steps from (*R*)-phenyloxirane and benzimidazole (see Supporting Information). The intended CIAT mechanism was investigated by reacting **16** with thionyl chloride in various solvents [MeCN, *i*PrOAc, MTBE, cyclopentyl methyl ether (CPME), 2-methyltetrahydrofuran (MeTHF), toluene, trifluorotoluene, and chlorobenzene] but proved unsuccessful. In most cases, the phosphonochloridate **17** did not crystallize from the reaction mixture or, when it did [in tetrahydrofuran (THF) and MeTHF], no significant diastereomeric enrichment was observed upon displacement with alanine.

Despite the unsuccessful attempts at obtaining enrichment via CIAT, we envisioned that the benzimidazole-derived chiral auxiliary could be leveraged in a DYKAT mechanism. Based on a precedent of phosphonamidate synthesis via DYKAT,[17a] reaction conditions were developed to access material enriched in up to 65:35 dr from phosphonic dichloride **20** by sequential treatment with **11** and phenol (Scheme 6). However, cleavage of the chiral auxiliary by hydrogenation revealed that the selectivity was in favor of the undesired (R_P)-diastereomer **19**. To exploit such stereochemical preference to our advantage, an alternative strategy was devised. Dichloride **20** was treated sequentially with **11** and an electron-poor phenol that could act as a leaving group (Scheme 7). As expected, mixtures enriched in (R_P)-diastereomer were obtained. Among the activated phenols that we tested (nitrophenols and pentafluorophenol), 3-nitrophenol gave the highest dr (65:35). The resulting phosphonamidate **21** was then treated with sodium phenoxide in DCM, affording the desired (S_P)-diastereomer **18** in 79:21 dr.

With a diastereoselective route to the desired (S_P)-diastereomer in hand, our attention turned to the final

Scheme 5. Use of Benzimidazole-Derived Chiral Auxiliary in a CIAT Process

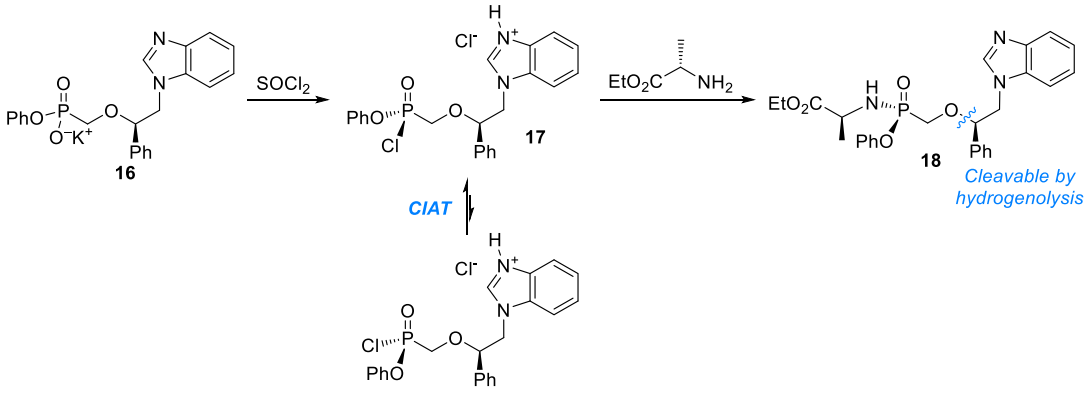

https://doi.org/10.1021/acs.oprd.0c00428
Org. Process Res. Dev. 2021, 25, 1247−1262

Scheme 6. Use of Benzimidazole-Derived Chiral Auxiliary in a DYKAT Process

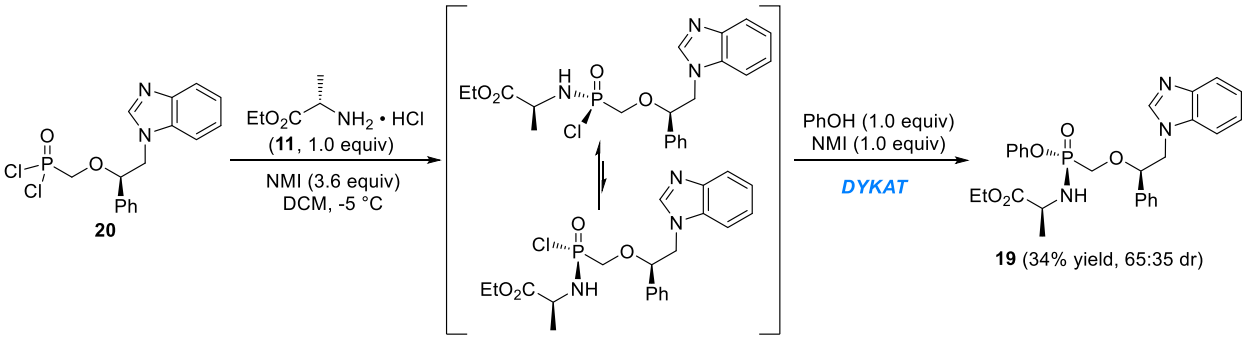

Scheme 7. Use of Benzimidazole-Derived Chiral Auxiliary in a DYKAT Process with 3-Nitrophenol

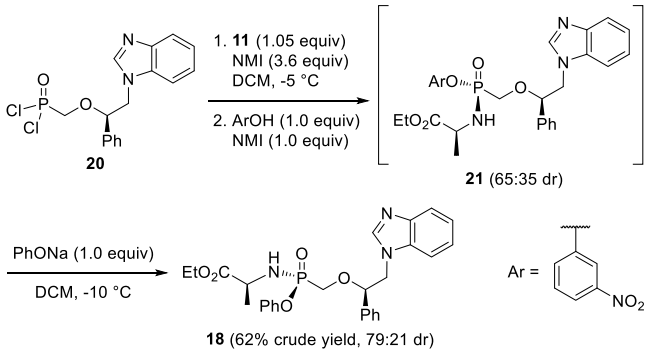

deprotection step. Contrary to our expectations, removal of the benzylic chiral auxiliary by hydrogenolysis was problematic. Full conversion of **18** to **1** could only be achieved with a high loading of a mixture of Pd/C and $Pd(OH)_2/C$ (76 mol % each), under 4 bar of H_2 at 60 °C over 6 days. Due to these challenges, chiral auxiliary routes were not further investigated.

Encouraged by the diastereoselectivity trends observed with the chiral auxiliary-bearing substrate **20**, we further evaluated DYKAT approaches using a variety of O- and/or N-substituted derivatives (Table 3). Initial attempts using *O*-benzyl phosphonic dichloride **22** and **11** provided the corresponding phosphonamidates in modest diastereomeric enrichment in favor of the undesired (R_P)-isomer (40:60 dr, entry 1). However, switching to *N*-benzyl Ala-OEt (**24**) as the nucleophile improved the dr to 74:26, favoring the (S_P)-isomer (entry 2). Interestingly, the diastereoselectivity is affected by the choice of the base for the individual additions. The highest (S_P)-selectivity was obtained with a mixture of *N*-methylimidozole (NMI) and triethylamine (TEA). When NMI alone was used in step 1, selectivity reversed to favor the (R_P)-isomer (34:66 dr; not listed). A more pronounced effect was also observed with 4-(dimethylamino) pyridine (DMAP) [20:80 dr, favoring (R_P), entry 3]. It is possible that nucleophilic, unhindered bases change the mechanism of substitution such that nucleophilic addition of the base to the phosphonamidyl chloride occurs prior to the addition of phenol. Unfortunately, these conditions were ineffective with the displaceable 4-nitrophenol nucleophile, providing little dr enhancement (41:59 dr, entry 4). In an effort to improve diastereoselectivity and/or obtain crystalline products whose dr could be further enhanced by crystallization, additional substitution patterns were investigated. Gratifyingly, it was found that the TsO-phosphonic dichloride **23**, combined with **24**, yields excellent levels of selectivity (96:4 dr), yet favoring the undesired (R_P)-diastereomer (entries 6−7). In contrast, reaction of **23** with unprotected alanine **11** resulted in lower selectivity (59:41 dr, entry 5). As previously accomplished

Table 3. DYKAT Sequence Using N- and O-Derivatives

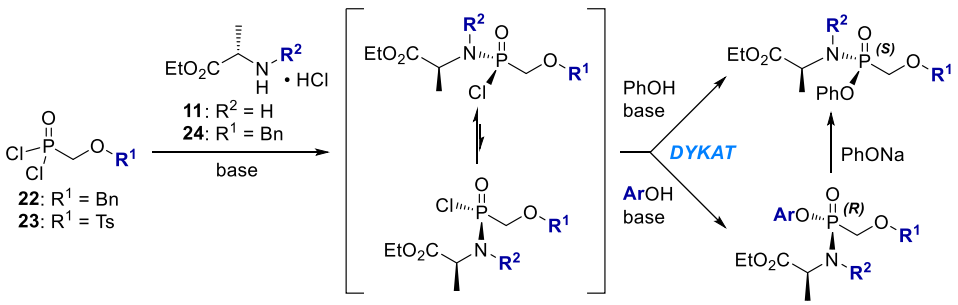

entry	R^1	R^2	step 1 conditions	Ar	step 2 conditions	$(S_P)/(R_P)$ dr[b]
1	Bn	H	NMI (2.2 equiv) MeCN, −5 to 22 °C	Ph	NMI (1.1 equiv) MeCN, −5 to 22 °C	40:60
2		Bn[a]	TEA (3.0 equiv) NMI (1.0 equiv) DCM, −5 °C	Ph	NMI (1.1 equiv) DCM, −5 to 22 °C	74:26
3		Bn[a]	DMAP (3.0 equiv) NMI (1.0 equiv) DCM, 0 to 22 °C	Ph	NMI (1.1 equiv) DCM, 0 to 22 °C	20:80
4		Bn[a]	DMAP (3.0 equiv) NMI (1.0 equiv) DCM, 0 to 22 °C	4-(NO_2)-C_6H_4	NMI (1.15 equiv) DCM, 0 to 22 °C	41:59
5	Ts	H	NMI (3.5 equiv) DCM/MeCN, 0 °C	Ph	NMI (1.0 equiv) DCM, 0 to 22 °C	59:41
6		Bn	NMI (3.5 equiv) DCM/MeCN, 0 °C	Ph	DCM, 0 to 22 °C	4:96
7		Bn	NMI (3.5 equiv) DCM/MeCN, 0 °C	3-(NO_2)-C_6H_4	DCM, 0 to 22 °C	4:96

[a]The free base of the alanine derivative was used. [b]Determined by UPLC or ^{31}P NMR.

https://doi.org/10.1021/acs.oprd.0c00428
Org. Process Res. Dev. 2021, 25, 1247−1262

with substrate **20**, the high (R_P)-selectivity could be turned to our advantage by carrying out the displacement with 3-nitrophenol (yielding **25**), followed by treatment with sodium phenolate (Scheme 8). Through this sequence, the desired (S_P)-isomer **26** was obtained in 85:15 dr.

Scheme 8. DYKAT Sequence Using Phosphonic Dichloride 23 and 3-Nitrophenol

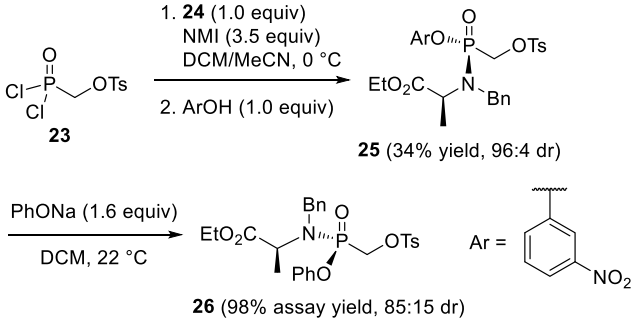

Unfortunately, challenges were encountered in the conversion of **26** to the unprotected phosphonamidate **1** by the removal of the protecting groups. Tosyl cleavage ($CeCl_3 \cdot H_2O$/NaI) or conversion to the *O*-benzyl derivative (TBAI/BnOH) could not be accomplished without decomposition of the relatively unstable phosphonamidate moiety. The *N*-benzyl group also proved difficult to be removed by hydrogenolysis. With the phosphonamidate derivative **15** (obtained through the conditions in Table 3, entry 2), complete hydrogenolytic cleavage of the *N*-benzyl group could only be achieved with a high loading of Pd/C and $Pd(OH)_2$/C (40 mol % each), under 4 bar of H_2 at 60 °C over 2 days. Given the unsuccessful conversion of **26** to **1** and the poor step/atom economy for other derivatives under analysis, we chose to deprioritize research into diastereoselective approaches.

2.3. Selective Crystallization. As the investigation of stereoselective phosphonamidate synthesis was unable to deliver a scalable, satisfactory alternative to SMB, our attention shifted to the selective crystallization of the desired diastereomer. Two opportunities exist in the current synthetic route for selective crystallization: (i) crystallization of the benzylated intermediate **12** (or an alternative, O-protected precursor), and (ii) crystallization of **1**. The former option is preferable due to the beneficial impact on PMI of positioning a low-yielding step earlier in the synthesis.[21]

2.3.1. Synthesis and Selective Crystallization of Benzylated Analogues. As **12** is a viscous liquid, research efforts focused on the identification of crystalline, benzyl-substituted analogues of **12** to be exploited in a selective crystallization process, or, more ambitiously, in a CIAT process. In order to be a practical alternative to SMB, the intended analogue must satisfy the following requirements: (i) be a crystalline, high-melting solid; (ii) undergo selective crystallization (or CIAT) to provide materials with high diastereomeric enrichment; (iii) contain a functionalized benzylic protecting group easily removable by hydrogenation; and (iv) generate a hydrogenation byproduct that is easily removed from **1**.

Benzylation of **1** with benzylic halides was identified as a quick strategy to provide access to a variety of analogues of **12** to be evaluated for their crystallinity and capacity of crystallizing selectively from the corresponding (R_P)-epimers. Hydroxymethyl phosphonates and related compounds are poor nucleophiles,[22] typically requiring hydride bases[23] or Ag_2O[24] to undergo alkylation with alkyl halides. However, such conditions resulted in the rapid decomposition of **1**, and alternative benzylation conditions (benzylic bromide and organic/inorganic base) were equally unsuccessful. Nonetheless, acid-catalyzed benzylation using trichloroacetimidates allowed for the preparation of several analogues (see Supporting Information, Table S3), four of which were found to be crystalline solids and chosen for further development (Table 4,

Table 4. Crystalline Analogues of 12 and 13

Entry	Backbone	R	Melting point (° C)
1	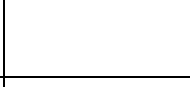	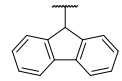 **27a**	118
2		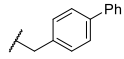 **27b**	79-81
3		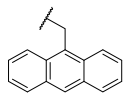 **27c**	140-144
4		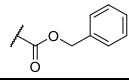 **27d**	53-54
5	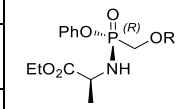	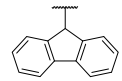 **28a**	88-91
6		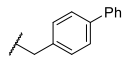 **28b**	51-54
7		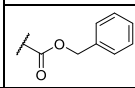 **28d**	69-72

entries 1−4). Three corresponding undesired phosphorus epimers (entries 5−7) were also synthesized to compare their crystalline properties and initiate studies of crystallization from mixtures of diastereomers.

2.3.1.1. 9-Fluorenyl and 4-Phenylbenzyl Analogues. In preparation for crystallization studies, we sought to determine the thermodynamic preference for either diastereomer under equilibrating conditions. Epimerization of **27a** with DBU/phenol was examined in several solvents (Table 5). A consistent ca. 50:50 dr was obtained after 4 days (entries 1−5). Epimerization of **28a** in DCM led to the same 50:50 dr (entry 6), thus confirming the lack of a thermodynamic preference for either diastereomer.

Subsequently, crystallization experiments were carried out to determine the possibility of enriching **27a** from a mixture of P-epimers (Table 6). Mixtures of **27a** and **28a** with a starting 74:26 dr were dissolved in a mixture of solvent/antisolvent and subjected to cooling crystallization (5 °C). Analysis of the crystallized solids showed improvement of the dr from 74:26 up to 98:2 (entries 1−4). However, when crystallization was attempted starting from a 51:49 mixture, no enrichment was observed (entries 5−8). The recovered solids were obtained as nearly 50:50 mixtures of diastereomers and were identified by XRPD as a new solid form (mp = 88−90 °C). Extensive solvent screening conducted on the new polymorph did not deliver any enrichment. These observations suggest the existence of the two diastereomers as a quasi-racemate[20b] that prevents selective crystallization of **27a** from a 1:1 mixture.

https://doi.org/10.1021/acs.oprd.0c00428
Org. Process Res. Dev. 2021, 25, 1247−1262

Table 5. Epimerization of 27a

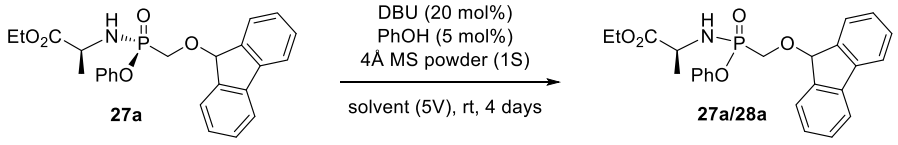

entry	substrate	solvent	dr (**27a**/**28a**)[a]
1	**27a**	DCM	50:50
2		THF	47:53
3		toluene	49:51
4		EtOAc	48:52
5		CH_3CN	48:52
6	**28a**	DCM	50:50

[a]Determined by UPLC.

Table 6. Selective Crystallization of 27a

entry	solvent	initial dr (**27a**/**28a**)[a]	final dr (**27a**/**28a**)[a]
1	THF/heptane 1:1	74:26	98:2
2	EtOAc/heptane 3:1		95:5
3	toluene/heptane 4:1		98:2
4	*i*PrOH/heptane 9:1		98:2
5	THF/heptane 2:3	51:49	55:45
6	toluene/heptane 4:1		47:53
7	MeTHF/heptane 1:1		49:51
8	MTBE/heptane 4:1		53:47

[a]Determined by UPLC.

Selective crystallization studies on the 4-phenylbenzyl analogue **27b** were executed in a similar fashion to **27a** and led to the same conclusions. Subjection of **27a** to standard epimerization conditions resulted in 50:50 dr, indicating the absence of a thermodynamic preference for either diastereoisomer. Moreover, selective crystallization trials from the dr = 49:51 input material resulted in no enrichment and detection of a new crystalline form by XRPD (mp = 74 °C).

2.3.1.2. 9-Anthracenylmethyl Analogue. As with **27a** and **27b**, the 9-anthracenylmethyl analogue **27c** was first subjected to epimerization conditions (Table 7). While the reaction in DCM returned the usual ca. 50:50 dr (entry 1), other solvents resulted in diastereomeric mixtures slightly favoring **27c** (entries 2−4).

Selective crystallization studies were next carried out, beginning from 80:20 and 50:50 mixtures of diastereomers (obtained by chromatographic purification of epimerized reaction mixtures). The solids were dissolved in a mixture of solvent/antisolvent and cooled to −3 °C (Table 8). Analysis of the crystallized solids showed that dr had improved to 99:1 when starting from an 80:20 mixture (entries 1−3) and to ≥91:9 when starting from a 50:50 mixture (entries 4−6).

Table 8. Selective Crystallization of 27c

entry	solvent	initial dr (**27c**/**28c**)[a]	final dr (**27c**/**28c**)[a]
1	EtOAc/heptane 2:1	80:20	99:1
2	*i*PrOH		99:1
3	THF/heptane 1:1		99:1
4	EtOAc/heptane 3:2	50:50	94:6
5	*i*PrOH/heptane 7:1		91:9
6	*i*PrOAc/heptane 7:2		92:8

[a]Determined by ^{31}P NMR.

The significant dr enrichment obtained during crystallization, along with the slight thermodynamic preference for the desired isomer **27c** in solution under equilibrating conditions, led us to believe that a CIAT process could be developed (Table 9). Thus, 51:49 **27c**/**28c** mixtures were subjected to standard epimerization conditions in several solvents in which **27c** has low solubility (<20 mg/g).[25] The suspensions were allowed to equilibrate for 1−4 days at the indicated temperature, the mixtures were then filtered, and the solids and mother liquors were analyzed for dr and % recovery. The high diastereomeric enrichment achieved (≥95:5, entries 1, 2, 5) and the >50% recovery suggest that a CIAT mechanism is indeed operative. Moreover, when the conditions of entry 6 were reproduced and the solvent was allowed to slowly evaporate over 3 days, the initial suspension fully converted to a crystalline solid of 95:5 dr. Unfortunately, high-yielding, nonevaporative reaction conditions could not be developed without experiencing a dr erosion (entries 4, 6, 7).

Table 7. Epimerization of 27c

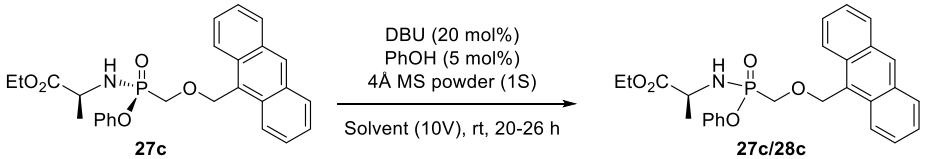

entry	solvent	dr (**27c**/**28c**)[a]
1	DCM	51:49
2	EtOAc	54:46
3	*i*PrOAc	58:42
4	*i*PrOAc/MTBE 7:3	68:32

[a]Determined by ^{31}P NMR.

https://doi.org/10.1021/acs.oprd.0c00428
Org. Process Res. Dev. 2021, 25, 1247−1262

Table 9. Optimization of CIAT Conditions

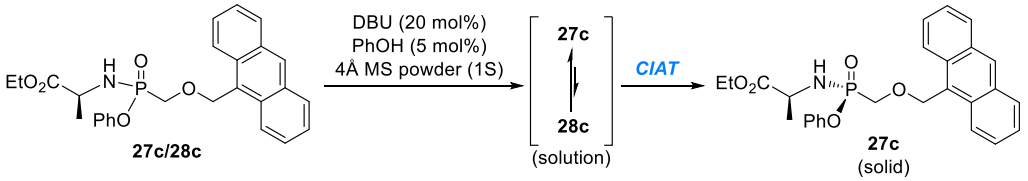

entry	solvent (amount)	T (°C)	solid recovery (%)[a]	solid dr (**27c**/**28c**)[b]	filtrate dr (**27c**/**28c**)[b]
1	*i*PrOAc (10 V)	21	46	97:3	54:45
2	*i*PrOAc (5 V)	21	57	95:5	75:25
4	*i*PrOAc (7 V)	−3	62	92:8	39:61
5	CPME (7 V)	21	50	95:5	52:48
6	MTBE (15 V)	21	64	88:12	25:75
7	*i*PrOAc (4 V), MTBE(2 V)	21	65	93:7	76:24

[a]Based on the total **27c**/**28c** input. [b]Determined by ^{31}P NMR.

Scheme 9. Hydrogenolysis of 27c

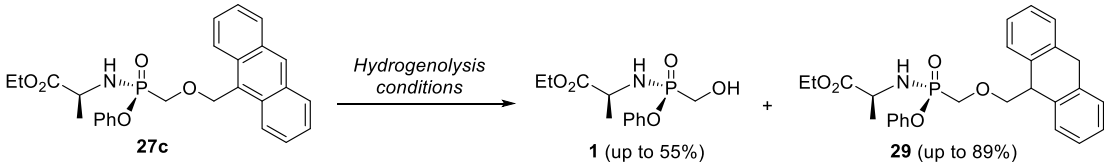

Concurrently, it was determined that the 9-anthracenylmethyl group cannot be removed easily under hydrogenolytic conditions due to the competing reduction of the 9,10-ring, resulting in >40% of compound **29** under most of the catalytic conditions screened (Scheme 9; see Supporting Information for additional details).

2.3.1.3. Benzyloxycarbonyl Analogue. Investigation of the selective crystallization of **27d** revealed that, unlike analogues **27a** and **27b**, a 1:1 mixture of diastereomers does not give rise to a new solid form, as determined by PXRD analysis. Moreover, solubility studies showed a striking difference between the two diastereomers in several solvents (Figure 3), with **27d** being typically more soluble than **28d**.

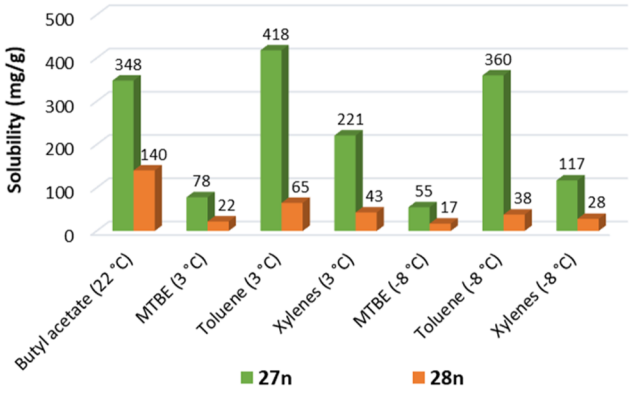

Figure 3. Solubility of **27d** and **28d**.

Selective crystallization experiments were executed to leverage the solubility difference and obtain diastereomerically enriched **27d** in the mother liquor. Mixtures of **27d**/**28d** with varying dr (53:47 to 62:38, favoring **27d**) were subjected to cooling crystallization in toluene and MTBE/toluene mixtures (Table 10). The dr value in the mother liquors was found to have improved up to 86:14 (entry 4). This behavior is in stark contrast with that of **27a** and **27b**, where no dr improvement upon crystallization was observed from ca. 50:50 mixtures. However, further experiments with toluene/MTBE solvent mixtures failed to provide crystallization conditions that could improve the dr above 85:15. Crystallization at this stage was therefore disregarded as potentially inefficient.

Table 10. Enrichment of 27d by Selective Crystallization of 28d

entry	solvent	T (°C)	initial dr (**27d**/**28d**)[a]	final dr (**27d**/**28d**)[a,b]
1	toluene	−8	62:38	75:25
2	toluene	−20	59:41	78:22
3	MTBE/toluene 2:1	−10	59:41	82:18
4	MTBE/toluene 2:1	−29	55:45	86:14
5	MTBE/toluene 1:1	−26	53:47	84:16

[a]Determined by ^{31}P NMR. [b]In the mother liquor.

2.3.2. Selective Crystallization of 1. **1** and its (R_P)-epimer (**30**) are both solid compounds. While **1** exhibits high crystallinity and a sharp melting point at 73−74 °C, **30** is a waxy solid melting at 38−40 °C. To develop a selective crystallization of **1**, its solubility was measured in various solvents at 22 °C (Figure 4). **1** displays low solubility (<40 mg/g) in aromatic hydrocarbons (toluene, *p*-xylene, and ethyl benzene), butyl esters (butyl acetate, isobutyl acetate, and *tert*-butyl acetate), and ethers (MTBE, CPME, *tert*-amyl methyl ether, diisopropyl ether, and dibutyl ether). A complementary solubility study using **30** was also performed with solvents in which **1** is poorly soluble. The solubility difference was found to be oftentimes remarkable, with **30** being approximately 20 times more soluble than **1** in ethers and 50 times more soluble in aromatic hydrocarbons.

With these data in hand, we felt confident that a cooling crystallization would allow us to isolate **1** in high yield and dr from a mixture of diastereomers. Among the solvents that

https://doi.org/10.1021/acs.oprd.0c00428
Org. Process Res. Dev. 2021, 25, 1247−1262

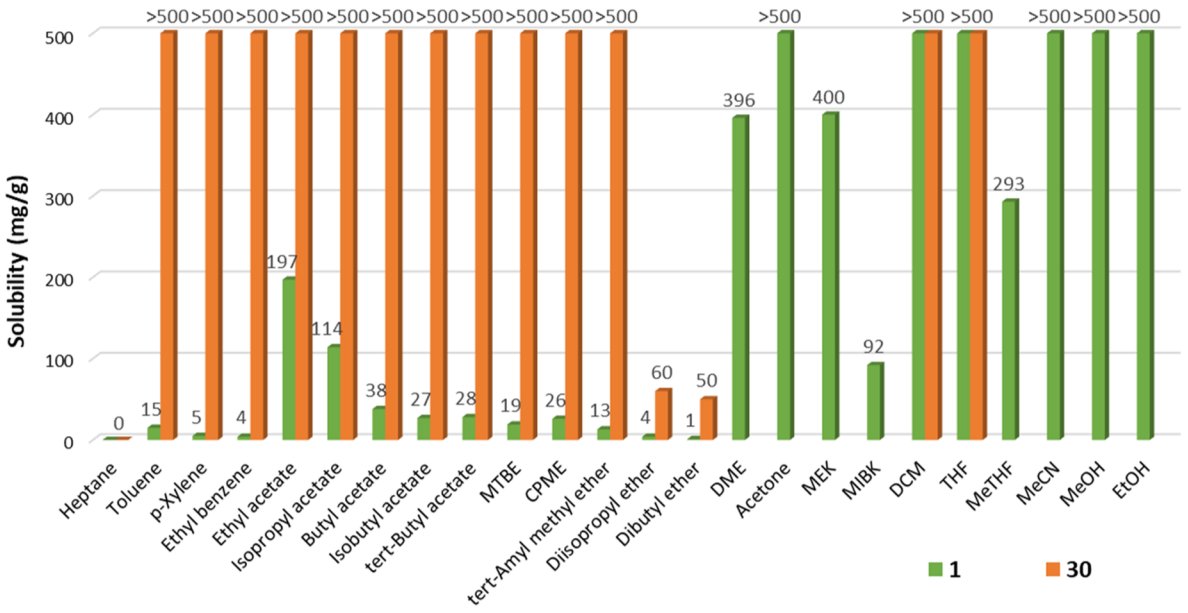

Figure 4. Solubility of **1** and **30** at 22 °C.

displayed high solubility difference, toluene, CPME, and MTBE were chosen for further investigation based on commercial availability, cost, and toxicity considerations.

Selective crystallization studies were performed by dissolving a 50:50 mixture of **1** and **30** in DCM and then exchanging the solvent to MTBE, CPME, or toluene (15 V). The slurries were cooled to −24 °C over 2 h and then aged for an additional 2 h. **1** was isolated by filtration and dried, and its purity/dr was determined by ^{31}P NMR (Table 11). Among the solvents tested, MTBE proved to be superior as it afforded **1** as a single diastereomer in high purity (entry 3).

Table 11. Selective Crystallization of 1

entry	solvent	yield (%)[a]	purity (% AN)[b]	solid dr (**1**/**30**)[b]	filtrate dr (**1**/**30**)[b]
1	toluene	70	94.0	94:6	76:24
2	CPME	64	95.2	97:3	77:23
3	MTBE	68	100	100:0	83:17

[a]Based on the maximum theoretical 50% yield. [b]Determined by ^{31}P NMR.

The MTBE selective crystallization conditions were then applied to a crude hydrogenolysis reaction mixture (Scheme 10). After hydrogenation of a mixture of **12** and **13** (44:56 dr), the DCM organic phase was filtered through a pad of Celite to remove the spent catalyst, followed by a water wash and solvent exchange to MTBE (5 V). The solution was cooled to −23 °C over 5 h and seeded with **1** (0.015 S) when the temperature reached 5 °C. After aging at −23 °C for 17 h, **1** was isolated by filtration in 32% yield and 96:4 dr.

Scheme 10. Selective Crystallization of 1 from the Hydrogenolysis Reaction Mixture

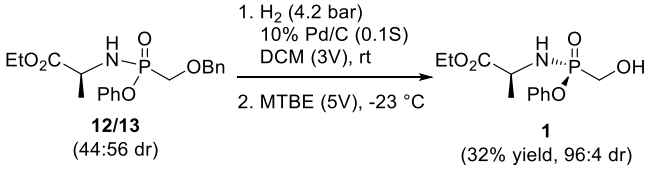

2.4. Second-Generation Synthesis. With reliable selective crystallization conditions in hand, a fully updated sequence to **1** was developed (Scheme 11). It was envisioned that moving to the benzyloxycarbonyl (Cbz) protecting group would eliminate the problematic use of BOMCl, while still accommodating the hydrogenolytic protecting group removal at the end of the synthesis. In addition, the Cbz group should be much easier to re-install than the benzyl group on **30**[26] to support a recycling strategy via the DBU/PhOH conditions.[27]

Scheme 11. Proposed Second-Generation Synthesis

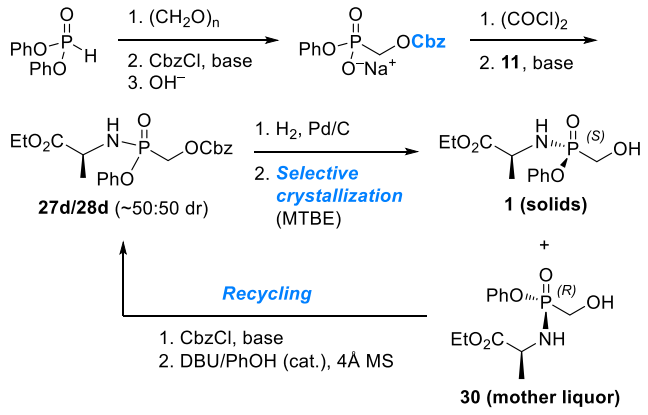

The synthesis begins with a five-step, telescoped sequence starting from diphenyl phosphite (Scheme 12). Notably, commercial sources of diphenyl phosphite contain variable amounts of phenol (4−20 mol %) and triphenyl phosphite (2−4 mol %), so any reaction conditions must be able to accommodate these impurities. Silylation of diphenyl phosphite using BSTFA, followed by Abramov reaction with paraformaldehyde at 90 °C provided the silyl ether **32** (Table 12, entry 1). Whereas silyl phosphites react readily with simple aliphatic aldehydes at room temperature,[28] reactions of phosphonates (other than methyl) with paraformaldehyde typically require

https://doi.org/10.1021/acs.oprd.0c00428
Org. Process Res. Dev. 2021, 25, 1247−1262

Scheme 12. Telescoped Abramov/Cbz Protection/Hydrolysis Sequence

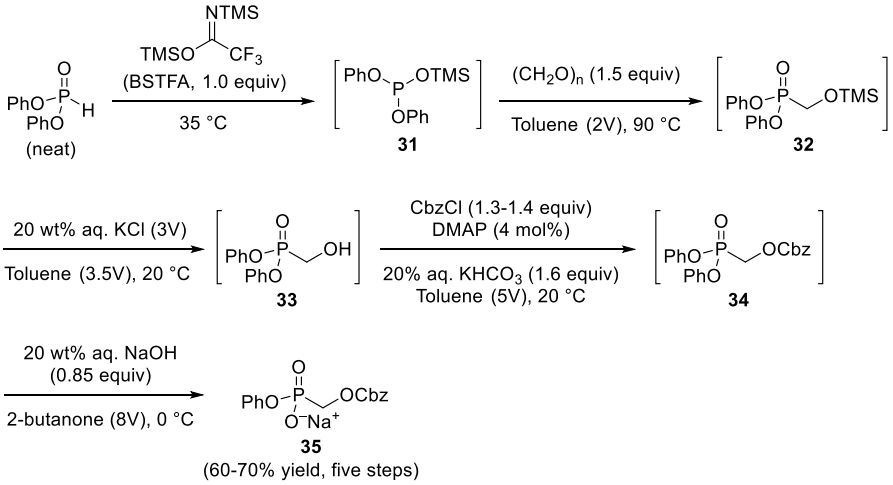

Table 12. Evaluation of Conditions for Silylation and Abramov Reaction of Diphenyl Phosphite

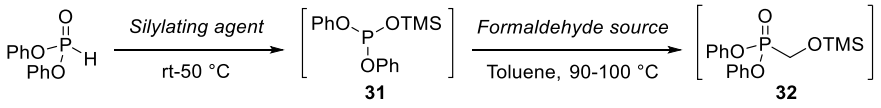

entry	silylation conditions	Abramov conditions	conversion to **31** (%)[a]	conversion to **32** (%)[a]
1	BSTFA (1.0 equiv) neat, 35 °C	$(CH_2O)_n$ (1.5 equiv) toluene (2 V), 90 °C	99.7	>99.9
2	BSTFA (1.0 equiv) neat, 35 °C	trioxane (0.5 equiv) toluene (2 V), 90 °C	>99.9	0
3	BSA (1.0 equiv) neat, 50 °C	$(CH_2O)_n$ (1.5 equiv) toluene (2 V), 90 °C	93.5	26.4
4	TMSCl (1.0 equiv) Et_3N (1.0 equiv) toluene (8 V), rt	$(CH_2O)_n$ (1.0 equiv), 100 °C	89.6	3.8

[a]Determined by ^{31}P NMR.

more forcing conditions.[29] Trioxane was investigated as an alternative source of formaldehyde, but it failed completely to react in the Abramov reaction (entry 2). In addition, while more common silylating reagents such as *N,O*-bis(trimethylsilyl)-acetamide (BSA) or TMSCl are effective for the formation of **31**, the Abramov reaction proceeds poorly when these reagents are used (entries 3 and 4).

Desilylation to the hydroxymethylphosphonate **33** was initially accomplished by methanol treatment and removal of the volatile methoxytrimethylsilane under vacuum. However, hydrolysis to release phenol occurred to a varying extent and led to reduced yields. More reproducible conditions were later identified under biphasic conditions, where the presence of potassium chloride helped to minimize hydrolysis.

Attention then turned to Cbz protection. Acylation conditions involving stoichiometric triethylamine and catalytic DMAP led to a complex reaction mixture (Table 13, entry 1). Subsequent stability studies indicated that **33** readily decomposes when treated with alkyl amines and is only moderately stable to DMAP. Instead, pyridine was identified as a suitable base to carry out the protection reaction. However, reaction screening with varying amounts of pyridine and CbzCl revealed that the reaction tends to stall with a maximum of ca. 60% conversion (entries 2 and 3). NMR analysis showed that this is due to in situ decomposition of CbzCl to benzyl chloride, which can be suppressed by moving to a more nonpolar solvent and utilizing slow addition of CbzCl (entries 4 and 5). Alternatively, the Cbz protection could be completed under Schotten–Baumann conditions using the more benign potassium bicarbonate as the base (entry 6). Indeed, these conditions were found to streamline nicely with the aqueous desilylation

Table 13. Evaluation of Conditions for Cbz Protection of 33

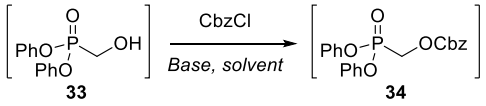

entry	conditions	**34** (% AN)[a]
1	CbzCl (1.5 equiv), DMAP (0.1 equiv), Et_3N (1.5 equiv), DCM (10 V), 0 °C to rt	0 (decomp.)
2	CbzCl (1.0 equiv), pyridine (1.0 equiv), DCM (10 V), rt	58.8
3	CbzCl (1.2 equiv), pyridine (2.0 equiv), DCM (10 V), rt	54.1
4	pyridine (2.0 equiv), toluene (15 V), 0 °C, CbzCl (1.1 equiv, charged over 20 min)	87.5
5	pyridine (2.0 equiv), toluene (15 V), 0 °C, CbzCl (1.1 equiv, charged over 60 min)	96.0
6	CbzCl (1.0 equiv), DMAP (2 mol %), 10 wt % aq. $KHCO_3$ (1.3 equiv), toluene (5 V), rt	97.3
7	CbzCl (1.3 equiv), DMAP (4 mol %), toluene (5 V), rt, 20 wt % aq. $KHCO_3$, (1.5 equiv, charged over 40 min)	97.7 (91% assay yield)

[a]Determined by ^{31}P NMR.

conditions and could be completed from the same biphasic mixture. The best results were obtained with slow addition of aqueous potassium bicarbonate, which helps to minimize the hydrolytic degradation of **33** (entry 7).

Finally, the solution of **34** is solvent-exchanged into 2-butanone and subjected to monohydrolysis conditions using aqueous sodium hydroxide. A substoichiometric amount of hydroxide (0.85 equiv) was found to be optimal to limit bis-hydrolysis. After reaction completion, azeotropically distilling the mixture at a constant volume with replacement of 2-

https://doi.org/10.1021/acs.oprd.0c00428
Org. Process Res. Dev. 2021, 25, 1247−1262

butanone until the water content is below 1.5 wt % allows the sodium salt **35** to crystallize directly from the reaction mixture. The process is capable of purging phenol and other impurities that were generated throughout the processing and typically provides **35** in 60−70% yield (over 5 steps) and >95% purity.

The phosphonamidate moiety is installed subsequently from **35** through a two-step telescoped process (Scheme 13). In the first step, Vilsmeier conditions are used to access the corresponding phosphonochloridate **36**, which is treated in the second step with **11** and DIPEA to obtain a mixture of phosphonamidate diastereomers **27d**/**28d**. In the chlorination step, a slight excess of oxalyl chloride is required to achieve full conversion and avoid the unproductive formation of phosphonyl anhydrides **37**. However, the excess oxalyl chloride is detrimental in the subsequent displacement step with **11** as it leads to the formation of a bis-oxalyl alanine impurity **38**. To overcome this challenge, a distillation step was introduced after chlorination to remove excess oxalyl chloride. As expected, the purity profile and yield of the telescoped sequence displayed variability depending on the water content of **11** and DIPEA. To increase the robustness of the process, it became necessary to predry solutions of **11** and DIPEA in DCM with TMSCl prior to their addition to a DCM solution of **36**. With the optimized chlorination/displacement conditions, the diastereomeric mixture of **27d**/**28d** is obtained as a DCM solution in 85−97% assay yield over two steps. Interestingly, the coupling reaction reliably proceeds with ≥55:45 dr in favor of the desired (S_P)-diastereomer **27d**. In contrast, in the previous manufacturing route, the *O*-Bn-protected-phosphonochloridate **10** undergoes displacement providing 45:55 dr in favor of the undesired (R_P)-diastereomer **13**. The explanation for the switch in diastereoselectivity based on the protecting group is not clear at this time.

Scheme 13. Telescoped Chlorination/Displacement Sequence and Final Hydrogenolysis Step

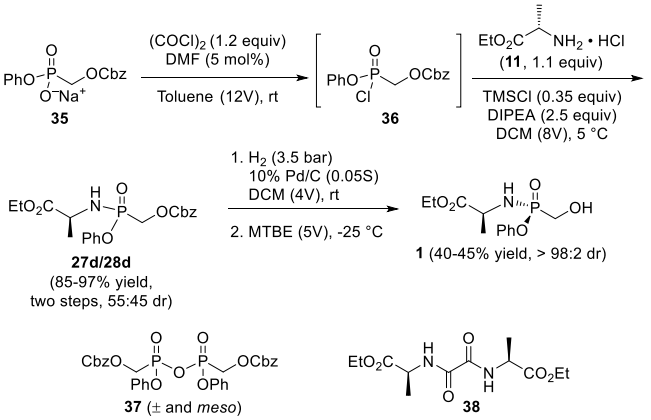

In the final step, the DCM solution of **27d**/**28d** is subjected to hydrogenolysis using 10% Pd/C under 3.5 bar of hydrogen. In comparison to the benzyl group deprotection in the previous route, the Cbz deprotection requires half the catalyst loading (0.05 vs 0.1 S, or 2 vs 4 mol %), proceeds in a much shorter reaction time (6 h vs ca. 3 days), and affords a cleaner reaction profile. The selective crystallization process discussed in Section 2.3.2 was successfully applied for the isolation of **1** in 40−45% yield and >98:2 dr.

To demonstrate the scalability of the route, the sequence was performed at 3 kg diphenylphosphite input scale (Scheme 14). The initial five-step telescoped sequence resulted in 3.06 kg of **35** (78% yield corrected for the purity of diphenyl phosphite, 95.7% AN purity). 500 g of **35** was carried through the chlorination/displacement sequence, obtaining the phosphonamidate intermediates **27d**/**28d** as a DCM solution in 85% yield (56:44 dr, 98.2% AN purity). Finally, hydrogenolysis and selective crystallization afforded 164 g of **1** as a white crystalline solid in 46% yield and 99.4:0.6 dr (99.5% AN purity).

3. CONCLUSIONS

In summary, stereoselective synthesis, selective crystallization, and epimer recycling were extensively evaluated to access **1** in an expeditious and cost-effective manner. Ultimately, the switch from SMB to selective crystallization and the introduction of the Cbz protecting group enabled access to an improved synthetic route (Table 14). Although both first- and second-generation routes entail a sequence of eight steps with two solid-state isolations, the second-generation route proceeds with a higher overall yield (36% increase) and lower PMI (16% reduction).

Contrary to our expectations, analysis of PMI metrics revealed that solvent usage remains unaltered in the second-generation route (approximately 200 kg of solvents per kg of **1**, Figure 5). The solvent-saving opportunity offered by the removal of SMB from the sequence appears to be offset by the increased solvent demand of step 1. However, the usage of raw materials and water is significantly reduced on a kg/kg basis due to the combined effect of several factors: high yields for all steps, favorable dr in step 2, and lack of solvent exchange operations involving water. Thanks to these improvements, cost and lead time of **1** are estimated to decrease by 50% on a manufacturing scale.

Scheme 14. Second-Generation Route to Phosphonamidate 1

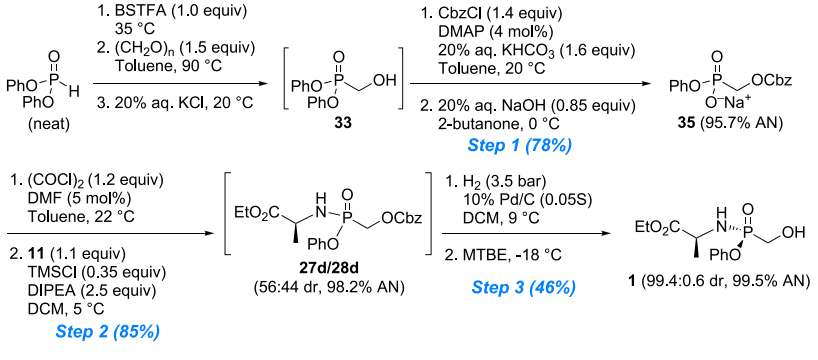

https://doi.org/10.1021/acs.oprd.0c00428
Org. Process Res. Dev. 2021, 25, 1247−1262

Table 14. Comparison of First- and Second-Generation Routes

attribute		first-generation route	second-generation route
synthetic steps		8 (4 manufacturing steps, 2 isolations)	8 (3 manufacturing steps, 2 isolations)
diastereomer resolution		SMB	selective crystallization
overall yield		22	30
PMI	*total*	328	275
	reactants/reagents	45	16
	solvents	198	201
	water	85	58
lead time		5 months	2.5 months

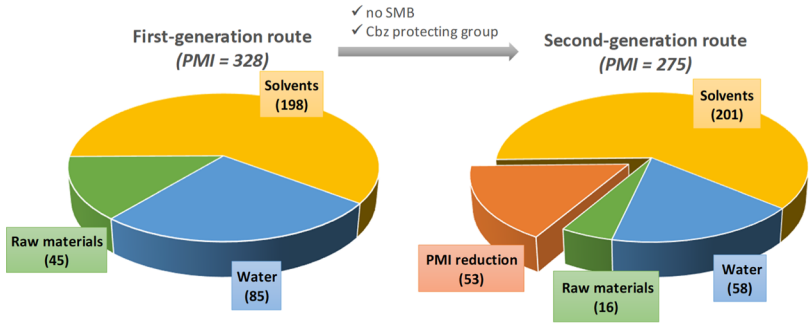

Figure 5. Comparison of PMI breakdown for first- and second-generation routes.

4. EXPERIMENTAL SECTION

4.1. General Experimental. All substrates and reagents were commercially available and used as received. Diphenyl phosphite was obtained from Millipore-Sigma with approximately 86% w/w purity, as determined by ^{1}H NMR using 1,3,5-trimethoxybenzene as an internal reference. NMR spectroscopy was performed on a Bruker Ascend 400 (400 MHz) system, using $CDCl_3$, DMSO-d_6, or D_2O as the solvent. For NMR analysis, 200 μL of the reaction solution or 20 mg solid was added to 0.75 mL of the deuterated solvent. UPLC analysis was performed using a Waters Acquity UPLC system as follows: (i) Chiral purity of **27d**/**28d**: Waters Acquity BEH Phenyl column (1.7 μm, 2.1 × 100 mm) with 0.4 mL/min flow rate and 30 °C column temperature. The analytical method utilized two mobile phases: mobile phase A consisted of 0.1% (v/v) formic acid in H_2O and mobile phase B consisted of MeOH. The gradient elution method was completed as follows: 1.0 min 35% of mobile phase B; 6.0 min 55% mobile phase B; 16.0 min 75% mobile phase B; 18.0 min 90% mobile phase B; 20.0 min 90% mobile phase B; and 20.1 min 35% mobile phase B. The eluting material was detected using a UV detector set at 207 nm. (ii) Purity of **1**: Waters Acquity UPLC HSS T3 column (1.8 μm, 2.1 × 100 mm) with 0.5 mL/min flow rate and 25 °C column temperature. The analytical method utilized two mobile phases: mobile phase A consisted of 0.1% (v/v) formic acid in H_2O and mobile phase B consisted of MeCN. The gradient elution method was completed as follows: 2.0 min 3% of mobile phase B; 15.0 min 90% mobile phase B; 17.0 min 90% mobile phase B; 17.1 min 3% mobile phase B; and 22.0 min 3% mobile phase B. The eluting material was detected using a UV detector set at 260 nm. (iii) Chiral purity of **1**: CHIRALPAK IC-3 column (3 μm, 4.6 × 150 mm) with 0.4 mL/min flow rate of isocratic elution of 7:3 TFA (0.1% v/v) in water/*i*PrOH at 40 °C column temperature over 30 min. The eluting material was detected using a UV detector set at 260 nm.

4.2. Sodium Phenyl[(benzyloxycarbonyloxy)methyl]-phosphonate (35). A 16 L, jacketed glass-lined reactor was charged with diphenyl phosphite (3.02 kg, 12.9 mol, 1.0 equiv) and warmed to an internal temperature of 35 °C. BSTFA (3.29 kg, 12.8 mol, 1.0 equiv) was added dropwise over 45 min while maintaining the temperature of the batch at 35 °C, and the mixture was aged for 30 min and then sampled for conversion to **31**. ^{31}P NMR (162 MHz, $CDCl_3$): δ 124.2 ppm (92.9% AN). Paraformaldehyde (0.57 kg, 18.9 mol, 1.5 equiv) and toluene (6.5 L, 2.2 V) were added, and the batch was ramped linearly to 90 °C over a period of 2 h. The mixture was aged for an additional 2 h and then sampled for conversion to **32**. ^{31}P NMR (162 MHz, $CDCl_3$): δ 16.3 ppm (93.8% AN). The batch was cooled to 20 °C and diluted with aq. potassium chloride (20 wt %, 9.0 L, 3.0 V) and toluene (10.6 L, 3.5 V). After stirring for 15 h, the organic layer was sampled for conversion to **33**. ^{31}P NMR (162 MHz, $CDCl_3$): δ 18.0 ppm (93.6% AN). 4-Dimethylaminopyridine (60.5 g, 0.03 equiv) and benzyl chloroformate (3.09 kg, 18.1 mol, 1.4 equiv) were added, followed by a slow addition of aq. potassium bicarbonate over 30−60 min (20 wt %, 10.2 kg, 1.6 equiv). The mixture was aged for an additional 60 min and then sampled for conversion to **34**. ^{31}P NMR (162 MHz, $CDCl_3$): δ 11.1 ppm (96.6% AN). The phases were allowed to settle, the aqueous layer was separated, and the organic layer was washed with aq. sodium chloride (5 wt %, 6.0 L, 2.0 V). The resulting organic layer was concentrated *in vacuo* with a maximum jacket temperature of 50 °C to a final volume of ca. 6 L (2.0 V); then, 2-butanone (12.0 L, 4.0 V) was added, and the batch was re-distilled to ca. 6 L. 2-Butanone (18.0 L, 6.0 V) was added, and the mixture was sampled to ensure that the toluene content was below 10 wt % (relative to 2-butanone) and then cooled to an internal temperature of 0 °C. Aq. sodium hydroxide (20 wt %, 2.09 kg, 0.8 equiv) was charged dropwise over ca. 60 min, and the mixture was stirred for 30 min and then sampled for conversion to **35**. ^{31}P NMR (162 MHz, $CDCl_3$): δ 0.9 ppm (95.7% AN). Aq. HCl (18.5 wt %) was charged until the solution pH was ca. 7 (required 0.16 kg, 0.06 equiv), and the batch was warmed to an internal temperature of 22 °C. 2-Butanone (39.2 L, 13.0 V) was charged followed by **35** seed crystals (15.0 g,

https://doi.org/10.1021/acs.oprd.0c00428
Org. Process Res. Dev. 2021, 25, 1247−1262

0.003 equiv), and the slurry was aged for 15 min. With a maximum jacket temperature of 55 °C, the batch was distilled under vacuum while maintaining a constant volume via addition of 2-butanone, until the Kf of the mother liquor was NMT 1.5% (required 32.8 L of fresh 2-butanone, 10.9 V). The batch was then cooled to 22 °C over 1 h, filtered, washed with 2-butanone (15.0 L, 5.0 V), and dried under vacuum at 45 °C for 20 h to provide 3.06 kg of **35** as a white solid (95.7% AN purity by ^{31}P NMR, 78% yield corrected for purity of diphenyl phosphite). ^{1}H NMR (400 MHz, DMSO-d_6): δ 7.41−7.29 (m, 5H), 7.25−7.17 (m, 2H), 7.12−7.04 (m, 2H), 7.03−6.95 (m, 1H), 5.09 (s, 2H), 4.12 (d, J = 8.3 Hz, 2H) ppm. ^{13}C NMR (101 MHz, D_2O): δ 155.2 (d, J = 9.6 Hz), 151.4 (d, J = 7.7 Hz), 134.8, 129.6 (d, J = 1.1 Hz), 128.5, 128.4, 128.2, 124.2 (d, J = 1.1 Hz), 120.8 (d, J = 3.7 Hz), 70.1, 61.7 (d, J = 160.3 Hz) ppm. ^{31}P NMR (162 MHz, DMSO-d_6): δ 6.3 ppm. HRMS $[M + H]^+$: calcd for $C_{15}H_{16}O_6P$, 323.0684; found, 323.0685; $[M - H]^-$: calcd for $C_{15}H_{14}O_6P$, 321.0528; found, 321.0533.

4.3. Ethyl (*S*)-[(Benzyloxycarbonyloxy)methyl](phenoxy)phosphoryl-L-alaninate (27d) and Ethyl (*R*)-[(Benzyloxycarbonyloxy)methyl](phenoxy)phosphoryl-L-alaninate (28d). A three-neck, 2 L round-bottom flask was charged with oxalyl chloride (0.22 kg, 1.70 mol, 1.2 equiv) and toluene (0.58 L, 1.2 V). A 15 L jacketed glass-lined reactor was charged with **35** (0.50 kg, 1.46 mol, 1.0 equiv), DMF (5.36 g, 7.3 mmol, 0.05 equiv), and toluene (5.2 L, 10.4 V). DCM (0.38 L, 0.8 V) was charged via a spray head. The reactor contents were adjusted to 15 °C, and the oxalyl chloride/toluene solution was added slowly over 2 h while maintaining the temperature of the batch at 25 °C. The resulting slurry was aged at 22 °C for 20 h and then sampled for conversion to the monochloridate **36**. ^{31}P NMR (162 MHz, $CDCl_3$): δ 26.2 ppm (100% AN). The reactor contents were distilled under vacuum with a maximum jacket temperature of 40 °C to a final volume of ca. 1.5 L (3.0 V). The temperature was adjusted to 22 °C, and DCM (0.7 L, 1.4 V) was added via a spray head. A three-neck, 3 L round-bottom flask was charged with **11** (0.25 kg, 1.59 mol, 1.1 equiv) and DCM (2.7 L, 5.4 V). After aging for 15 min at room temperature, chlorotrimethylsilane (39 g, 0.36 mol, 0.25 equiv) was added, and the solution was aged for 20 h. A three-neck, 3 L round-bottom flask was charged with DIPEA (0.47 kg, 3.64 mol, 2.5 equiv), DCM (0.38 L, 0.8 V), chlorotrimethylsilane (16 g, 0.15 mol, 0.1 equiv), and toluene (0.29 L, 0.6 V) and aged for 2 h at room temperature. The solution of **11** in DCM was charged to the reactor containing the monochloridate **36** over 30 min, and the mixture was aged for 1 h at 22 °C. The reactor contents were adjusted to 5 °C, and the DIPEA/DCM/toluene solution was added slowly over 2 h while maintaining the temperature of the batch at 10 °C. After aging for 1 h at 5 °C, the mixture was sampled for conversion to **27d**/**28d**. UPLC: 95.52% AN, 55:45 (S_P)/(R_P). Water (2.5 L, 5.0 V) and MTBE (3.4 L, 6.8 V) were charged while keeping the internal temperature at 25 °C. The reactor contents were adjusted to 22 °C and aged for 15 min. The phases were allowed to settle, the aqueous layer was separated, and the organic layer was washed sequentially with aq. K_2CO_3 (0.25 M, 2.5 kg, 5.0 S), twice with aq. HCl (0.1 M, 2.5 kg, 5.0 S), and water (2.5 kg, 5.0 S). The resulting organic layer was concentrated under vacuum with a maximum jacket temperature of 40 °C to a final volume of ca. 0.8 L (1.6 V). DCM (1.1 L, 2.2 V) was added via a spray head. The reactor contents were concentrated under vacuum until the distillation stalled, and a dark mobile oil was obtained. DCM (2.3 L, 4.6 V) was added, and the reactor contents were adjusted to 22 °C. 3.30 kg of **27d**/**28d** was obtained as a 15.9 wt % stock solution in DCM [98.16% AN purity by UPLC, 85.4% assay yield, 55:45 (S_P)/(R_P)]. For characterization purposes, **27d** and **28d** were obtained by chromatographic purification of a portion of the DCM solution. Data for **27d**: ^{1}H NMR (400 MHz, $CDCl_3$): δ 7.40−7.35 (m, 5H), 7.32−7.27 (m, 2H), 7.20−7.13 (m, 3H), 5.22−5.16 (m, 2H), 4.57 (dd, J = 14.2, 9.0 Hz, 1H), 4.47 (dd, J = 14.2, 7.1 Hz, 1H), 4.20−4.02 (m, 3H), 3.66 (t, J = 10.6 Hz, 1H), 1.30 (d, J = 7.1 Hz, 3H), 1.19 (t, J = 7.1 Hz, 3H). ^{13}C NMR (101 MHz, $CDCl_3$): δ 173.4 (d, J = 5.6 Hz), 154.7 (d, J = 10.4 Hz), 149.8 (d, J = 8.5 Hz), 134.7, 129.8, 128.8, 128.6, 128.5, 125.2 (d, J = 0.9 Hz), 120.5 (d, J = 4.6 Hz), 70.5, 62.2 (d, J = 156.8 Hz), 61.5, 49.7, 21.3 (d, J = 4.1 Hz), 14.0. ^{31}P NMR (162 MHz, $CDCl_3$): δ 17.9 ppm. HRMS $[M + H]^+$: calcd for $C_{20}H_{25}O_7NP$, 422.1363; found, 422.1360. Data for **28d**: ^{1}H NMR (400 MHz, $CDCl_3$): δ 7.41−7.34 (m, 5H), 7.31−7.27 (m, 2H), 7.19−7.13 (m, 3H), 5.23−5.16 (m, 2H), 4.54 (d, J = 8.0 Hz, 2H), 4.18−4.05 (m, 1H), 4.12 (q, J = 7.2 Hz, 1H), 4.11 (q, J = 7.2 Hz, 1H), 3.60 (t, J = 10.5 Hz, 1H), 1.31 (d, J = 7.1 Hz, 3H), 1.22 (t, J = 7.1 Hz, 3H). ^{13}C NMR (101 MHz, $CDCl_3$): δ 173.6 (d, J = 5.8 Hz), 154.7 (d, J = 10.1 Hz), 149.7 (d, J = 8.6 Hz), 134.7, 129.7, 128.7, 128.6, 128.5, 125.1 (d, J = 1.3 Hz), 120.6 (d, J = 4.7 Hz), 70.4, 61.8 (d, J = 155.3 Hz), 61.5, 49.6 (d, J = 1.8 Hz), 21.3 (d, J = 4.2 Hz), 14.0. ^{31}P NMR (162 MHz, $CDCl_3$): δ 18.9 ppm. HRMS $[M + H]^+$: calcd for $C_{20}H_{25}O_7NP$, 422.1363; found, 422.1361.

4.4. Ethyl (*S*)-(Hydroxymethyl) (phenoxy)phosphoryl-L-alaninate (1) and Ethyl (*R*)-(Hydroxymethyl) (phenoxy)phosphoryl-L-alaninate (30). A 1 L Parr reactor was charged with water-wet 10% Pd/C (26.15 g, 0.02 equiv) and a stock solution of **27d**/**28d** in DCM (3.30 kg solution, 0.52 kg **27d**/**28d**, 1.23 mol). After degassing, the reactor contents were adjusted to 9 °C and hydrogenated at 3.5 bar. After 5.5 h, the mixture was sampled for conversion to 1/30. ^{31}P NMR (162 MHz, $CDCl_3$): δ 26.1 ppm (43.8% AN, 30), 24.8 ppm (55.0% AN, 1). The mixture was filtered through a Buchner funnel coated with Celite (0.15 kg). The reactor and Celite pad were rinsed forward with DCM (2.9 L, 5.5 V). The filtrates were combined and transferred into a 5 L glass-lined reactor. The solution was concentrated under vacuum with a maximum jacket temperature of 30 °C to a final volume of ca. 0.8 L (1.5 V). The reactor contents were co-distilled with MTBE (2.7 L, 5.2 V) to a final volume of ca. 0.8 L (1.5 V). MTBE (2.7 L, 5.2 V) was charged to the reactor, and the mixture was sampled for the determination of toluene content by ^{1}H NMR. Co-distillation with MTBE was repeated until the toluene content with respect to MTBE was 2.5 mol % or less. The reactor contents were adjusted to 30 °C and ramp-cooled to −18 °C over 5 h. The mixture was seeded with **1** (7.8 g, 0.02 equiv) when the internal temperature reached 10 °C. The mixture was aged at −18 °C for 14 h, filtered, and the cake was rinsed with MTBE (0.2 L, 0.4 V) precooled at −18 °C . The wet cake was dried under vacuum at 20 °C for 5 h to provide 0.164 kg of **1** as a white solid [99.52% AN purity by UPLC, 46.1% yield, 99.4:0.6 (S_P)/(R_P)]. ^{1}H NMR (400 MHz, $CDCl_3$): δ 7.31 (dd, J = 8.6, 7.2 Hz, 2H), 7.22 (dt, J = 8.7, 1.3 Hz, 2H), 7.18−7.11 (m, 1H), 4.15 (q, J = 7.1 Hz, 2H), 4.09−4.01 (m, 1H), 4.01 (dd, J = 14.8, 5.5 Hz, 1H), 3.96 (dd, J = 14.8, 5.2 Hz, 1H), 3.86 (br s, 1H), 3.40 (br s, 1H), 1.34 (d, J = 7.0 Hz, 3H), 1.24 (t, J = 7.2 Hz, 3H). ^{13}C NMR (101 MHz, $CDCl_3$): δ 174.2 (d, J = 4.7 Hz), 150.2 (d, J = 9.2 Hz), 129.6, 124.8, 120.5 (d, J = 4.6 Hz), 61.5, 58.2 (d, J = 149.8 Hz), 49.6, 20.9 (d, J = 4.5 Hz), 14.0. ^{31}P NMR (162 MHz, $CDCl_3$): δ 24.8 ppm. HRMS $[M + H]^+$: calcd for $C_{12}H_{19}O_5NP$, 288.0995; found, 288.0993. For characterization purposes, **30** was

https://doi.org/10.1021/acs.oprd.0c00428
Org. Process Res. Dev. 2021, 25, 1247−1262

obtained as a white solid after chromatographic purification of the mother liquor. ^{1}H NMR (400 MHz, $CDCl_3$): δ 7.36−7.27 (m, 2H), 7.22 (dt, J = 8.6, 1.3 Hz, 2H), 7.20−7.11 (m, 1H), 4.20−4.11 (m, 1H), 4.17 (q, J = 7.1 Hz, 2H), 4.00 (dd, J = 14.9, 6.9 Hz, 1H), 3.93 (dd, J = 14.9, 2.9 Hz, 1H), 3.48 (br s, 1H), 3.17 (br s, 1H), 1.37 (d, J = 7.2 Hz, 3H), 1.26 (t, J = 7.2 Hz, 3H). ^{13}C NMR (101 MHz, $CDCl_3$): δ 174.9 (d, J = 4.3 Hz), 150.0 (d, J = 9.2 Hz), 129.5, 124.8 (d, J = 1.2 Hz), 120.7 (d, J = 4.4 Hz), 61.6, 58.0 (d, J = 147.6 Hz), 49.5 (d, J = 1.2 Hz), 20.8 (d, J = 4.8 Hz), 13.9. ^{31}P NMR (162 MHz, $CDCl_3$): δ 26.1 ppm. HRMS [M + H]$^+$: calcd for $C_{12}H_{19}O_5NP$, 288.0995; found, 288.0995.

■ ASSOCIATED CONTENT

Supporting Information

The Supporting Information is available free of charge at https://pubs.acs.org/doi/10.1021/acs.oprd.0c00428.

General procedures, experimental details, synthesis of starting materials, and NMR data (PDF)

■ AUTHOR INFORMATION

Corresponding Author

Andrea Ambrosi − *Process Chemistry, Gilead Sciences Inc., Foster City, California 94404, United States;* orcid.org/0000-0002-2889-5913; Email: andrea.ambrosi@gilead.com

Authors

Dustin A. Bringley − *Process Chemistry, Gilead Sciences Inc., Foster City, California 94404, United States*

Selcuk Calimsiz − *Process Development, Gilead Alberta ULC, Edmonton, Alberta T6S 1A1, Canada*

Jeffrey A. O. Garber − *Process Development, Gilead Alberta ULC, Edmonton, Alberta T6S 1A1, Canada*

Huy Huynh − *Process Development, Gilead Alberta ULC, Edmonton, Alberta T6S 1A1, Canada*

Sankar Mohan − *Process Development, Gilead Alberta ULC, Edmonton, Alberta T6S 1A1, Canada*

Keshab Sarma − *Process Chemistry, Gilead Sciences Inc., Foster City, California 94404, United States*

Jinyu Shen − *Process Development, Gilead Alberta ULC, Edmonton, Alberta T6S 1A1, Canada*

Jonah Curl − *Process Development, Gilead Alberta ULC, Edmonton, Alberta T6S 1A1, Canada*

Bernard Kwong − *Process Development, Gilead Alberta ULC, Edmonton, Alberta T6S 1A1, Canada*

Olga Lapina − *Process Chemistry, Gilead Sciences Inc., Foster City, California 94404, United States*

Edmund Leung − *Process Development, Gilead Alberta ULC, Edmonton, Alberta T6S 1A1, Canada*

Lennie Lin − *Process Development, Gilead Alberta ULC, Edmonton, Alberta T6S 1A1, Canada*

Andrew Martins − *Process Development, Gilead Alberta ULC, Edmonton, Alberta T6S 1A1, Canada*

Teague McGinitie − *Analytical Chemistry, Gilead Alberta ULC, Edmonton, Alberta T6S 1A1, Canada*

Jaspal Phull − *Process Development, Gilead Alberta ULC, Edmonton, Alberta T6S 1A1, Canada*

Ben Roberts − *Process Chemistry, Gilead Sciences Inc., Foster City, California 94404, United States*

Mary Rosario − *Process Development, Gilead Alberta ULC, Edmonton, Alberta T6S 1A1, Canada*

Bing Shi − *Process Chemistry, Gilead Sciences Inc., Foster City, California 94404, United States*

Eric A. Standley − *Process Chemistry, Gilead Sciences Inc., Foster City, California 94404, United States*

Li Wang − *Process Development, Gilead Alberta ULC, Edmonton, Alberta T6S 1A1, Canada*

Xueqing Wang − *Process Development, Gilead Alberta ULC, Edmonton, Alberta T6S 1A1, Canada*

Guojun Yu − *Process Development, Gilead Alberta ULC, Edmonton, Alberta T6S 1A1, Canada*

Complete contact information is available at: https://pubs.acs.org/10.1021/acs.oprd.0c00428

Notes

The authors declare the following competing financial interest(s): The authors are employees of Gilead Sciences, Inc., Foster City, California, USA, and Gilead Alberta ULC, Edmonton, Alberta, Canada.

■ ACKNOWLEDGMENTS

The authors are grateful to Amy Cagulada, Nisha Shah, Elan Shao, and Mark Smith for performing reaction safety assessments, Alban Pereira and Alejandro Corona for assistance with obtaining characterization data, and Chiajen Lai for helpful discussion on selective crystallization.

■ REFERENCES

(1) (a) Pertusati, F.; Serpi, M.; McGuigan, C. Medicinal Chemistry of Nucleoside Phosphonate Prodrugs for Antiviral Therapy. *Antiviral Chem. Chemother.* **2012**, *22*, 181−203. (b) Pradere, U.; Garnier-Amblard, E. C.; Coats, S. J.; Amblard, F.; Schinazi, R. F. Synthesis of Nucleoside Phosphate and Phosphonate Prodrugs. *Chem. Rev.* **2014**, *114*, 9154−9218. (c) Slusarczyk, M.; Serpi, M.; Pertusati, F. Phosphoramidates and phosphonamidates (ProTides) with antiviral activity. *Antiviral Chem. Chemother.* **2018**, *26*, 204020661877524. (d) Mehellou, Y.; Rattan, H. S.; Balzarini, J. The ProTide Prodrug Technology: From the Concept to the Clinic. *J. Med. Chem.* **2018**, *61*, 2211−2226.

(2) (a) Ballatore, C.; McGuigan, C.; De Clercq, E.; Balzarini, J. Synthesis and evaluation of novel amidate prodrugs of PMEA and PMPA. *Bioorg. Med. Chem. Lett.* **2001**, *11*, 1053−1056. (b) Chapman, H.; Kernan, M.; Prisbe, E.; Rohloff, J.; Sparacino, M.; Terhorst, T.; Yu, R. Practical synthesis, separation, and stereochemical assignment of the PMPA pro-drug GS-7340. *Nucleosides, Nucleotides Nucleic Acids* **2001**, *20*, 621−628. (c) Pertusati, F.; Hinsinger, K.; Flynn, Á. S.; Powell, N.; Tristram, A.; Balzarini, J.; McGuigan, C. PMPA and PMEA prodrugs for the treatment of HIV infections and human papillomavirus (HPV) associated neoplasia and cancer. *Eur. J. Med. Chem.* **2014**, *78*, 259−268. (d) Ray, A. S.; Fordyce, M. W.; Hitchcock, M. J. M. Tenofovir alafenamide: A novel prodrug of tenofovir for the treatment of Human Immunodeficiency Virus. *Antiviral Res.* **2016**, *125*, 63−70.

(3) (a) Cihlar, T.; Ray, A. S.; Boojamra, C. G.; Zhang, L.; Hui, H.; Laflamme, G.; Vela, J. E.; Grant, D.; Chen, J.; Myrick, F.; White, K. L.; Gao, Y.; Lin, K.-Y.; Douglas, J. L.; Parkin, N. T.; Carey, A.; Pakdaman, R.; Mackman, R. L. Design and Profiling of GS-9148, a Novel Nucleotide Analog Active against Nucleoside-Resistant Variants of Human Immunodeficiency Virus Type 1, and Its Orally Bioavailable Phosphonoamidate Prodrug, GS-9131. *Antimicrob. Agents Chemother.* **2008**, *52*, 655−665. (b) Mackman, R. L.; Ray, A. S.; Hui, H. C.; Zhang, L.; Birkus, G.; Boojamra, C. G.; Desai, M. C.; Douglas, J. L.; Gao, Y.; Grant, D.; Laflamme, G.; Lin, K.-Y.; Markevitch, D. Y.; Mishra, R.; McDermott, M.; Pakdaman, R.; Petrakovsky, O. V.; Vela, J. E.; Cihlar, T. Discovery of GS-9131: Design, synthesis and optimization of amidate prodrugs of the novel nucleoside phosphonate HIV reverse transcriptase (RT) inhibitor GS-9148. *Bioorg. Med. Chem.* **2010**, *18*, 3606−3617.

(4) Standley, E. A.; Bringley, D. A.; Calimsiz, S.; Ng, J. D.; Sarma, K.; Shen, J.; Siler, D. A.; Ambrosi, A.; Chang, W.-T. T.; Chiu, A.; Davy, J. A.; Doxsee, I. J.; Esanu, M. M.; Garber, J. A. O.; Kim, Y.; Kwong, B.; Lapina, O.; Leung, E.; Lin, L.; Martins, A.; Phoenix, J.; Phull, J.; Roberts, B. J.; Shi, B.; St-Jean, O.; Wang, X.; Wang, L.; Wright, N.; Yu, G. Synthesis of Rovafovir Etalafenamide (Part I): Active Pharmaceutical Ingredient Process Development, Scale-Up, and Impurity Control Strategy. *Org. Process Res. Dev.* **2021**.

(5) Yu, R. H. C.; Brown, B. H.; Polniaszek, R. P.; Graetz, B. R.; Sujino, K.; Tran, D. D.-P.; Triman, A. S.; Kent, K. M.; Pfeiffer, S. Processes and intermediates for preparing anti-HIV agents. WO 2012159047 A1, 2012.

(6) (a) Curzons, A. D.; Mortimer, D. N.; Constable, D. J. C.; Cunningham, V. L. So you think your process is green, how do you know?—Using principles of sustainability to determine what is green—a corporate perspective. *Green Chem.* **2001**, *3*, 1–6. (b) Jimenez-Gonzalez, C.; Ponder, C. S.; Broxterman, Q. B.; Manley, J. B. Using the Right Green Yardstick: Why Process Mass Intensity Is Used in the Pharmaceutical Industry To Drive More Sustainable Processes. *Org. Process Res. Dev.* **2011**, *15*, 912–917.

(7) The hydrolysis of phosphonamidates **12**/**13** to yield **14** is an extremely facile reaction in the presence of trace amounts of base and water.

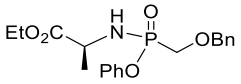

12/13

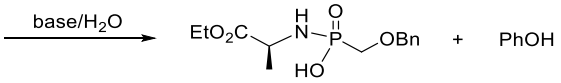

14

(8) (a) Cox, J. R.; Ramsay, O. B. Mechanisms of Nucleophilic Substitution in Phosphate Esters. *Chem. Rev.* **1964**, *64*, 317–352. (b) Harger, M. J. P. An elimination-addition mechanism for some phosphonamidic chloride-amine reactions. *Tetrahedron Lett.* **1981**, *22*, 4741–4742. (c) Harger, M. J. P. Evidence for elimination–addition mechanisms in the reactions of *N*-t-butyl-*P*-alkylphosphonamidic chlorides with t-butylamine and isopropylamine. *J. Chem. Soc., Perkin Trans. 1* **1983**, 2127–2131. (d) Freeman, S.; Harger, M. J. P. Associative and dissociative mechanisms for the reactions of *N*-t-butyl-*P*-phenylphosphonamidic chloride with isopropylamine and t-butylamine: competitive, kinetic, and stereochemical studies. *J. Chem. Soc., Perkin Trans. 2* **1988**, 81–90.

(9) van Bochove, M. A.; Swart, M.; Bickelhaupt, F. M. Nucleophilic Substitution at Phosphorus (SN2@P): Disappearance and Reappearance of Reaction Barriers. *J. Am. Chem. Soc.* **2006**, *128*, 10738–10744.

(10) (a) Kaljurand, I.; Kütt, A.; Sooväli, L.; Rodima, T.; Mäemets, V.; Leito, I.; Koppel, I. A. Extension of the Self-Consistent Spectrophotometric Basicity Scale in Acetonitrile to a Full Span of 28 pKa Units: Unification of Different Basicity Scales. *J. Org. Chem.* **2005**, *70*, 1019–1028. (b) Garrido, G.; Koort, E.; Ràfols, C.; Bosch, E.; Rodima, T.; Leito, I.; Rosés, M. Acid–Base Equilibria in Nonpolar Media. Absolute pKa Scale of Bases in Tetrahydrofuran. *J. Org. Chem.* **2006**, *71*, 9062–9067. (c) Rõõm, E.-I.; Kütt, A.; Kaljurand, I.; Koppel, I.; Leito, I.; Koppel, I. A.; Mishima, M.; Goto, K.; Miyahara, Y. Brønsted Basicities of Diamines in the Gas Phase, Acetonitrile, and Tetrahydrofuran. *Chem.—Eur. J.* **2007**, *13*, 7631–7643.

(11) Hanusek, J.; Hejtmánková, L.; Štěrba, V.; Sedlák, M. Influence of substitution on kinetics and mechanism of ring transformation of substituted S-[1-phenylpyrrolidin-2-on-3-yl]isothiuronium salts. *Org. Biomol. Chem.* **2004**, *2*, 1756–1763.

(12) (a) Lee, W. A.; He, G.-X.; Eisenberg, E.; Cihlar, T.; Swaminathan, S.; Mulato, A.; Cundy, K. C. Selective Intracellular Activation of a Novel Prodrug of the Human Immunodeficiency Virus Reverse Transcriptase Inhibitor Tenofovir Leads to Preferential Distribution and Accumulation in Lymphatic Tissue. *Antimicrob. Agents Chemother.* **2005**, *49*, 1898–1906. (b) Sofia, M. J.; Bao, D.; Chang, W.; Du, J.; Nagarathnam, D.; Rachakonda, S.; Reddy, P. G.; Ross, B. S.; Wang, P.; Zhang, H.-R.; Bansal, S.; Espiritu, C.; Keilman, M.; Lam, A. M.; Steuer, H. M. M.; Niu, C.; Otto, M. J.; Furman, P. A. Discovery of a β-d-2′-Deoxy-2′-α-fluoro-2′-β-C-methyluridine Nucleotide Prodrug (PSI-7977) for the Treatment of Hepatitis C Virus. *J. Med. Chem.* **2010**, *53*, 7202–7218.

(13) Pertusati, F.; McGuigan, C. Diastereoselective synthesis of P-chirogenic phosphoramidate prodrugs of nucleoside analogues (ProTides) via copper catalysed reaction. *Chem. Commun.* **2015**, *51*, 8070–8073.

(14) Roman, C. A.; Balzarini, J.; Meier, C. Diastereoselective Synthesis of Aryloxy Phosphoramidate Prodrugs of 3′-Deoxy-2′,3′-didehydrothymidine Monophosphate. *J. Med. Chem.* **2010**, *53*, 7675–7681.

(15) Xiang, D. F.; Bigley, A. N.; Desormeaux, E.; Narindoshvili, T.; Raushel, F. M. Enzyme-Catalyzed Kinetic Resolution of Chiral Precursors to Antiviral Prodrugs. *Biochemistry* **2019**, *58*, 3204–3211.

(16) Steinreiber, J.; Faber, K.; Griengl, H. De-racemization of Enantiomers versus De-epimerization of Diastereomers—Classification of Dynamic Kinetic Asymmetric Transformations (DYKAT). *Chem.—Eur. J.* **2008**, *14*, 8060–8072.

(17) (a) Cavalier, J.-F.; Fotiadu, F.; Verger, R.; Buono, G. New Highly Diastereoselective Synthesis of Phosphoramidates. A Route to Chiral Methyl *p*-Nitrophenyl Alkylphosphonates. *Synlett* **1998**, 73–75. (b) Tran, K.; Beutner, G. L.; Schmidt, M.; Janey, J.; Chen, K.; Rosso, V.; Eastgate, M. D. Development of a Diastereoselective Phosphorylation of a Complex Nucleoside via Dynamic Kinetic Resolution. *J. Org. Chem.* **2015**, *80*, 4994–5003. (c) Wang, L.; Cao, S.; Du, Z.; Wu, Q.; Bian, Z.; Kang, C.; Gao, L.; Zhang, J. 4-Dimethylaminopyridine-catalyzed dynamic kinetic resolution in asymmetric synthesis of *P*-chirogenic 1,3,2-oxazaphospholidine-2-oxides. *RSC Adv.* **2016**, *6*, 89665–89670. (d) Cini, E.; Barreca, G.; Carcone, L.; Manetti, F.; Rasparini, M.; Taddei, M. Stereoselective Synthesis of Sofosbuvir through Nucleoside Phosphorylation Controlled by Kinetic Resolution. *Eur. J. Org. Chem.* **2018**, 2622–2628.

(18) (a) Liu, S.; Zhang, Z.; Xie, F.; Butt, N. A.; Sun, L.; Zhang, W. First catalytic enantioselective synthesis of *P*-stereogenic phosphoramides via kinetic resolution promoted by a chiral bicyclic imidazole nucleophilic catalyst. *Tetrahedron: Asymmetry* **2012**, *23*, 329–332. (b) Wang, L.; Du, Z.; Wu, Q.; Jin, R.; Bian, Z.; Kang, C.; Guo, H.; Ma, X.; Gao, L. Organocatalytic Enantioselective Synthesis of *P*-Stereogenic Chiral Oxazaphospholidines. *Eur. J. Org. Chem.* **2016**, 2024–2028. (c) DiRocco, D. A.; Ji, Y.; Sherer, E. C.; Klapars, A.; Reibarkh, M.; Dropinski, J.; Mathew, R.; Maligres, P.; Hyde, A. M.; Limanto, J.; Brunskill, A.; Ruck, R. T.; Campeau, L.-C.; Davies, I. W. A multifunctional catalyst that stereoselectively assembles prodrugs. *Science* **2017**, *356*, 426–430.

(19) Ross, B. S.; Ganapati Reddy, P.; Zhang, H.-R.; Rachakonda, S.; Sofia, M. J. Synthesis of Diastereomerically Pure Nucleotide Phosphoramidates. *J. Org. Chem.* **2011**, *76*, 8311–8319.

(20) (a) Anderson, N. G. Developing Processes for Crystallization-Induced Asymmetric Transformation. *Org. Process Res. Dev.* **2005**, *9*, 800–813. (b) Brands, K. M. J.; Davies, A. J. Crystallization-Induced Diastereomer Transformations. *Chem. Rev.* **2006**, *106*, 2711–2733.

(21) Anderson, N. G. Route Selection. In *Practical Process Research & Development*; Anderson, N. G., Ed.; Academic Press: San Diego, 2000; pp 27–52.

(22) Gelat, F.; Lacomme, C.; Berger, O.; Gavara, L.; Montchamp, J.-L. Synthesis of (phosphonomethyl)phosphinate pyrophosphate analogues via the phospha-Claisen condensation. *Org. Biomol. Chem.* **2015**, *13*, 825–833.

(23) (a) Zhou, X.; Reilly, J. E.; Loerch, K. A.; Hohl, R. J.; Wiemer, D. F. Synthesis of isoprenoid bisphosphonate ethers through C–P bond formations: Potential inhibitors of geranylgeranyl diphosphate synthase. *Beilstein J. Org. Chem.* **2014**, *10*, 1645–1650. (b) Berger, O.; Montchamp, J.-L. General synthesis of *P*-stereogenic compounds: the menthyl phosphinate approach. *Org. Biomol. Chem.* **2016**, *14*, 7552–7562. (c) Mary, F.; Arrachart, G.; Leydier, A.; Pellet-Rostaing, S. Synthesis of organophosphorus ligands with a central oxygen atom and their applications in solvent extraction. *Tetrahedron* **2019**, *75*, 3968–3976.

https://doi.org/10.1021/acs.oprd.0c00428
Org. Process Res. Dev. 2021, 25, 1247–1262

(24) Wei, Y.; Qiu, G.; Lei, B.; Qin, L.; Chu, H.; Lu, Y.; Zhu, G.; Gao, Q.; Huang, Q.; Qian, G.; Liao, P.; Luo, X.; Zhang, X.; Zhang, C.; Li, Y.; Zheng, S.; Yu, Y.; Tang, P.; Ni, J.; Yan, P.; Zhou, Y.; Li, P.; Huang, X.; Gong, A.; Liu, J. Oral Delivery of Propofol with Methoxymethylphosphonic Acid as the Delivery Vehicle. *J. Med. Chem.* **2017**, *60*, 8580−8590.
(25) Solubility of **27m** in MTBE: 3 mg/g; CPME: 10 mg/g; *i*PrOAc: 16 mg/g.
(26) While re-benzylation of **30** would require use of benzyl trichloroacetimidate (Section 2.1), acylation with a carbamate protecting group is expected to be quite facile under mild conditions. See, for instance, Yan, B.; Spilling, C. D. Stereospecific Pd(O)-Catalyzed Malonate Additions to Allylic Hydroxy Phosphonate Derivatives: A Formal Synthesis of (−)-Enterolactone. *J. Org. Chem.* **2004**, *69*, 2859−2862.
(27) Recycling must involve reprotection of **30**. Attempts at direct epimerization of **30** resulted in its rapid decomposition when exposed to DBU.
(28) Engel, R. Phosphorus Addition at sp^2 Carbon. *Org. React.* **1988**, *36*, 175−248.
(29) (a) Kiyokawa, K.; Suzuki, I.; Yasuda, M.; Baba, A. Synthesis of Cyclopropane-Containing Phosphorus Compounds by Radical Coupling of Butenylindium with Iodo Phosphorus Compounds. *Eur. J. Org. Chem.* **2011**, 2163−2171. (b) Padilha, G.; Kaufman, T. S.; Silveira, C. C. Wittig−Horner mediated synthesis of 4-vinyl sulfide derivatives of pyrazoles. *Tetrahedron Lett.* **2016**, *57*, 3349−3353.

https://doi.org/10.1021/acs.oprd.0c00428
Org. Process Res. Dev. 2021, 25, 1247−1262